STAT3 controls the long-term survival and phenotype of repair Schwann cells during nerve regeneration

JNeurosci
THE JOURNAL OF NEUROSCIENCE

Research Articles: Development/Plasticity/Repair

STAT3 controls the long-term survival and phenotype of repair Schwann cells during nerve regeneration

Cristina Benito[+], Catherine M Davis[*,+], Jose A. Gomez-Sanchez, Mark Turmaine, Dies Meijer[1], Valeria Poli[2], Rhona Mirsky and Kristjan R Jessen

[1]Department of Cell and Developmental Biology, University College London, Gower Street, London WC1E 6BT, United Kingdom

[1]Centre for Neuroregeneration, The Chancellor's Building, 49 Little France Crescent, Edinburgh EH16 4SB, United Kingdom

[2]Department of Molecular Biotechnology and Health Sciences, University of Turin

DOI: 10.1523/JNEUROSCI.3481-16.2017

Received: 10 November 2016

Revised: 11 January 2017

Accepted: 19 January 2017

Published: 20 March 2017

Author contributions: C.B., C.M.D., R.M., and K.R.J. designed research; C.B., C.M.D., J.G.-S., M.T., and R.M. performed research; C.B., J.G.-S., R.M., and K.R.J. analyzed data; C.B., R.M., and K.R.J. wrote the paper; D.M. and V.P. contributed unpublished reagents/analytic tools.

Conflict of Interest: The authors have no conflits of interest to declare

We thank Laura Feltri and Larry Wrabetz (State University of New York at Buffalo, Buffalo NY) for the gift of Mpz-Cre mice. We thank Ashwin Woodhoo (CIC bioGUNE, Bilbal, Spain) for dissection of E12 nerves for precursor cultures, and R Martini (University of Würzburg, Germany) for a gift of L1 antibodies.

[+]These authors contributed equally to the work

Corresponding authors: Kristjan R Jessen, Department of Cell and Developmental Biology, University College London, Gower Street, London WC1E 6BT, United Kingdom e-mail: k.jessen@ucl.ac.uk Rhona Mirsky, Department of Cell and Developmental Biology, University College London, Gower Street, London WC1E 6BT, United Kingdom e-mail: r.mirsky@ucl.ac.uk

Cite as: J. Neurosci ; 10.1523/JNEUROSCI.3481-16.2017

Title: STAT3 controls the long-term survival and phenotype of repair Schwann cells during nerve regeneration

Authors: Cristina Benito+, Catherine M Davis[*+], Jose A. Gomez-Sanchez, Mark Turmaine, Dies Meijer[1], Valeria Poli[2], Rhona Mirsky, Kristjan R Jessen

Department of Cell and Developmental Biology, University College London, Gower Street, London WC1E 6BT, United Kingdom

*Present address: Department of Anesthesiology and Perioperative Medicine, The Knight Cardiovascular Institute, Oregon Health and Science University, 3181 S.W. Sam Jackson Park Rd. Portland, Oregon 97239-3098, USA

[1] Centre for Neuroregeneration, The Chancellor's Building, 49 Little France Crescent, Edinburgh EH16 4SB, United Kingdom

[2]Department of Molecular Biotechnology and Health Sciences, University of Turin
Via Nizza 52, 10126 Torino, Italy
+ These authors contributed equally to the work

Submitting author: Kristjan R. Jessen, Department of Cell and Developmental Biology, University College London, Gower Street, London WC1E 6BT, United Kingdom e-mail: k.jessen@ucl.ac.uk

Corresponding authors: Kristjan R Jessen, Department of Cell and Developmental Biology, University College London, Gower Street, London WC1E 6BT, United Kingdom e-mail: k.jessen@ucl.ac.uk Rhona Mirsky, Department of Cell and Developmental Biology, University College London, Gower Street, London WC1E 6BT, United Kingdom e-mail: r.mirsky@ucl.ac.uk

Abbreviated title: STAT supports repair Schwann cells

50 pages, 1 table, 8 figures,

Abstract 246, Introduction 649, Discussion 1482

The authors have no conflits of interest to declare

Acknowledgements and funding

We thank Laura Feltri and Larry Wrabetz (State University of New York at Buffalo, Buffalo NY) for the gift of Mpz-Cre mice. We thank Ashwin Woodhoo (CIC bioGUNE, Bilbal, Spain) for dissection of E12 nerves for precursor cultures, and R Martini (University of Würzburg, Germany) for a gift of L1 antibodies.

This work was funded by a Wellcome Trust Programme grant to KR Jessen and R Mirsky (074665), and MRC Project grant to KR Jessen and R Mirsky (G0600967), and grant agreement No. HEALTH-F2-2008-201535 from the European Community (FP7/2007-3013). C Benito was funded by the Marie Curie Research Grants Scheme, grant (271927).

Abstract

After nerve injury, Schwann cells convert to a phenotype specialised to promote repair. But during the slow process of axonal regrowth, these repair Schwann cells gradually lose their regeneration-supportive features and eventually die. Although this is a key reason for the frequent regeneration failures in humans, the transcriptional mechanisms that control long-term survival and phenotype of repair cells have not been studied, and the molecular signalling underlying their decline is obscure. We show, in mice, that Schwann cell STAT3 has a dual role. It supports the long-term survival of repair Schwann cells and is required for the maintenance of repair Schwann cell properties. In contrast, STAT3 is less important for the initial generation of repair Schwann cells after injury. In repair Schwann cells, we find that Schwann cell STAT3 activation by Tyr705 phosphorylation is sustained during long-term denervation. STAT3 is required for maintaining autocrine Schwann cell survival signalling, and inactivation of Schwann cell STAT3 results in a striking loss of repair cells from chronically denervated distal stumps. STAT3 inactivation also results in abnormal morphology of repair cells and regeneration tracks, and failure to sustain expression of repair cell markers including Shh, GDNF and BDNF. Since Schwann cell development proceeds normally without STAT3, the function of this factor appears restricted to Schwann cells after injury. This identification of transcriptional mechanisms that support long-term survival and differentiation of repair cells will help identify, and eventually correct, the failures that lead to the deterioration of this important cell population.

Significance Statement

Although injured peripheral nerves contain repair Schwann cells that provide signals and spatial clues for promoting regeneration, the clinical outcome after nerve damage is frequently poor. A key reason for this is during the slow growth of axons through the proximal parts of injured nerves repair Schwann cells gradually lose regeneration-supporting

features and eventually die. Identification of signals that sustain repair cells is therefore an important goal. We have found that in mice the transcription factor STAT3 protects these cells from death and contributes to maintaining the molecular and morphological repair phenotype that promotes axonal regeneration. Defining the molecular mechanisms that maintain repair Schwann cells is an essential step towards developing therapeutic strategies that improve nerve regeneration and functional recovery.

Key words

Regeneration, denervation, nerve, Schwann, injury

Introduction

The regeneration of damaged nerves depends on the presence of living Schwann cells in the nerve distal to injury. These cells are derived from myelin and Remak cells, but have adopted a phenotype that is specialized for supporting nerve repair (Arthur Farraj et al., 2012; Jessen et al., 2015; Jessen and Mirsky, 2016). Repair Schwann cells form regeneration tracks (bands of Bungner) that guide axons to their targets, break down myelin both directly by myelin autophagy and indirectly by activation of the innate immune response and recruitment of macrophages, and they express trophic factors that support survival of injured neurons and axon growth (Chen et al., 2007; Arthur-Farraj et al., 2012; Fontana et al., 2012; Glenn and Talbot, 2013; Brosius Lutz and Barres, 2014; Gomez-Sanchez et al., 2015). These cells differ in molecular expression, morphology, function and transcriptional controls from immature Schwann cells in developing nerves (Jessen and Mirsky, 2016).

Although peripheral nerves respond in this strikingly adaptive fashion to damage, the clinical outcome after nerve injury in larger animals including humans is frequently poor (Alan, 2000; Lundborg, 2000; Höke, 2006). One of the main reasons is that during the slow growth of

axons through the more proximal parts of injured nerves, the more distal nerve, which is without axonal contact for extended periods, gradually loses the capacity to support regeneration (Sulaiman and Gordon, 2009, 2013; Scheib and Höke, 2013). Two factors are thought to contribute to this deterioration. One is the gradual death of chronically denervated Schwann cells (Weinberg and Spencer, 1978; Siironen et al., 1994; Li et al., 1998; Jonsson et al., 2013). The other is the reduction in expression of growth-supportive factors including GDNF (glial derived neurotrophic factor) and BDNF (brain derived neurotrophic factor) by the surviving cells (You et al., 1997; Höke et al., 2002; Michalski et al., 2008; Eggers et al., 2010). This fading of the repair Schwann cell phenotype and the accompanying loss of regenerative support provided by the distal nerve stump have been carefully analysed in rodent models of chronic denervation (Sulaiman and Gordon 2009). Identification of the molecular mechanisms that sustain the differentiation state of repair cells and support their continual survival is clearly a significant goal.

We have previously identified activation of the transcription factor c-Jun in Schwann cells as an important regulator of the reprogramming of myelin and Remak cells into repair Schwann cells (Arthur-Farraj et al., 2012; Jessen and Mirsky, 2016). But transcriptional mechanisms that control long term maintenance of these cells have not been studied. Here we show that the STAT3 is involved in supporting the survival of chronically denervated repair cells, and also in maintaining their characteristic gene expression and morphology.

STAT3 is typically activated by phosphorylation of conserved tyrosine 705 residue in the C-terminal domain, resulting in dimerization and translocation from the cytoplasm to the nucleus (Aaronson and Horvath, 2002). Signalling is generally mediated via the gp130 receptor complex and Janus kinases (JAKs). STAT3 can also be phosphorylated on serine 727, which in most often serves to augment signalling initiated by tyrosine 705 phosphorylation (Decker and Kovarik, 2000).

STAT3 has previously been implicated in the injury response of CNS glial cells, since it is important for the formation of the astrocyte glial scar (Wanner et al., 2013). In Schwann cells

STAT3 is also known to be phosphorylated after injury (Sheu et al., 2000; Lee et al., 2009a; Lee et al., 2009b) but the functional role of STAT3 activation in Schwann cells has not been investigated. In the present work, we have addressed this issue during nerve development, regeneration and after long term injury. While we do not find major function for STAT3 in Schwann cell development or myelination, we identify an important role in the maintenance of chronically denervated repair Schwann cells. STAT3 is therefore the second transcription factor, in addition to c-Jun, with a selective function in Schwann cells of injured adult nerves.

Materials and methods

Animals

Animal experiments conformed to UK Home Office guidelines under the supervision of UCL Biological Services. Sprague-Dawley rat pups of either sex were obtained from UCL Biological Services. Mice of either sex with specific deletion of the STAT3 gene in Schwann cells were obtained by crossing $STAT3^{f/f}$ mice (Alonzi et al., 2001) with P_0-Cre mice (Feltri et al., 2002; D'Antonio et al., 2006), or with Dhh-Cre mice (Jaegle et al., 2003) (for experiments in Figs 3D, 4C and 6A-E). P_0-Cre mice were provided by L. Feltri and L. Wrabetz. The resulting P_0-Cre^{+}/$STAT3^{f/wt}$ mice were crossed back to $STAT3^{f/f}$ mice to obtain P_0-Cre^{+}/STAT3f/f mice, referred to as STAT3 cKO mice in which STAT3 is deleted from Schwann cells. P_0-Cre^{-}/$STAT3^{f/f}$ littermates, referred to as WT, were controls.

Genotyping

DNA for genotyping was was extracted from ear or tail samples using the Hot Sodium Hydroxide and Tris method (HotSHot) as in (Gomez-Sanchez J. A. et al., 2015). For primers see Table 1.

Antibodies

P-STAT3-Ser727 and P-STAT3-Tyr705 antibodies, both from Cell Signaling Technology were used at 1:50 for immunohistochemistry and 1:2000 for Western blotting. Other antibodies for Western blotting were Cyclin D1 (1:200; Santa Cruz Biotechnology), N-Cadh (1:500; BD Transduction Laboratories), p75NTR (1:1000; Millipore), GAP43 (1:500; Millipore), c-Jun (1:1000; Cell Signaling Technology) and GAPDH (1:5,000; Sigma-Aldrich). HRP-conjugated secondary antibodies (1:2,000 in blocking solution) were from Cell Signaling Technology. For immunohistochemistry, incubation with MBP antibodies (1:10,000; COVANCE) or 324 rat anti-mouse Ig L1 antibodies (1:10) were followed by anti-mouse Ig Alexa Fluor 488 (1:500; Molecular Probes) or anti-rat Ig Alexa Fluor 488 (1:500; Molecular Probes), respectively. Incubation with antibodies to Ki67 (1:100; Abcam) and SOX10 (1:100; R&D Systems) were followed by biotinylated anti-rabbit IgG (1:600; Amersham Biosciences) and anti-goat Ig Alexa Fluor 488 (1:1000; Molecular Probes) antibodies, respectively. The Ki67 sections were then incubated with Alexa Fluor 488 Streptavidin (1:500; Molecular Probes). CASPASE3 antibody (1:100; Cell Signaling Technology) was followed by anti-rabbit Ig Cy3. S100 antibody (1:1000) was from Dako.

Nerve Injury

The right sciatic nerve was exposed and transected at the sciatic notch (Woodhoo et al., 2009), or crushed (3x15 sec at three rotation angles) using fine forceps. Contralateral uninjured sciatic nerves were used as controls.

Cell and segment cultures, BrdU assay, infection and transfection

Schwann cell cultures and BrdU assay were as in Morgan et al.,1991 (see also Survival assays). Mouse Schwann cells and Schwann cell precursors were prepaired as in Arthur-Farraj et al., 2011 and Jessen et al., 1994, respectively. The precursors were cultured in serum-free supplemented medium (Meier et al.,1999), referred to as DM (defined medium), containing 20 ng/ml βNRG-1. Tibial nerve segments were maintained in DMEM with 5% FBS (Gomez Sanchez et al., 2015). Adenoviral infections and plasmid transfections were as in

Parkinson et al. 2001; 2004. An adenovirus expressing Cre recombinase (Akagi et al., 1997) was used to infect $STAT3^{f/f}$ Schwann cells generating STAT3 KO cells. Constitutively active STAT3 plasmid (Bromberg et al., 1999), STAT3-CA, was provided by Dr A Stephanou (Institute of Child Health, UCL, London). The control used was the pRc/CMV empty vector (Invitrogen Life Technologies, Paisley, UK). Both were co-transfected with a pBabe-GFP plasmid to allow visualization of transfected cells. The STAT3 peptide inhibitor (Calbiochem) used in the proliferation assay is a cell permeable STAT3-SH2 domain-binding phosphopeptide that contains a C-terminal membrane translocating sequence, acting as a highly selective, potent blocker of STAT3 activation (Turkson, et al., 2001). The AG490 JAK2 kinase (STAT3) inhibitor was from Calbiochem.

Electron microscopy

Nerves were processed as previously described (Gomez-Sanchez et al., 2015). Transverse ultrathin sections of cut tibial nerves were taken 5 mm from the cut site. To analyse the structure of Bungner bands, 20-26 random photographs per nerve at X12K were used. For cell counts, nuclei counted in every field, or every second or every third field, depending on the size of the nerve, were mutiplied by the number of fields to generate totals. Regeneration tracks (Bungner`s bands) were identified as a group of Schwann cell profiles (sometimes a single profile) surrounded by a basal lamina sheath as seen in transverse nerve sections. Roundness index and profile area were obtained after manual tracing of randomly selected profiles using ImageJ software.

Survival assay

Schwann cells from P1 STAT3 cKO and WT mice were assayed as in Meier et al., 1999. Cells were plated at low density (200 cells/coverslip) or high density (3000 cells/coverslip. After 3 hr at 37ºC and 5% CO_2, one set of coverslips from each animal was fixed immediately for immunolabelling to obtain a reference point for the quantification of survival at later time points. The remaining sets were topped up with 400µl of defined simple

medium (sDM; Meier et al., 1999) alone or sDM containing 1.6 ng/ml IGF-II (Peprotech Ltd, London, UK), 0.8 ng/ml PDGF-BB (Peprotech Ltd) and 0.8 ng/ml NT-3 (Regeneron Pharmaceuticals), or conditioned medium, and cultured for 48 or 72 hr. Then, cells were fixed using 4% PFA (paraformaldehyde) for 10 min, labeled with S100 antibodies and Hoechst dye, and the number of surviving Schwann cells counted. Survival percentage is the number of living cells present at 48 and 72 hr as a percentage of the number of cells that had attached to the substrate in sister cultures at 3 hr. sDM consists of 1:1 DMEM and Ham's F-12 supplemented with bovine serum albumin (350 µg/ml). Schwann cell conditioned medium was prepared as previously described (Meier et al., 1999).

TUNEL staining

To detect apoptotic cells, DNA fragmentation was labelled using the terminal deoxynucleotide transferase-mediated dUTP-biotin nick end labeling (TUNEL) method , using TUNEL enzyme (Roche) and TUNEL Lab Mix (Roche), according to the manufacturer's protocol. To identify TUNEL positive nuclei from Schwann cells and macrophages, immunolabeling with S100 and F4/80 (1:100; AbD Serotec), respectively, was carried out subsequently. Nuclei were stained using Hoechst dye.

Western blotting and quantitative PCR

For blotting, homogenates were obtained from injured and uninjured nerves as well as cultured nerve segments essentially as previously (Gomez-Sanchez et al., 2015). Experiments were repeated at least three times with fresh samples and representative pictures are shown. Densitometric quantification was by Image Lab 4.1 (Bio-Rad Laboratories). Measurements were normalized to loading control GAPDH. For PCR, total RNA was isolated using the RNeasy Lipid Tissue Mini Kit (Qiagen) with a DNase I step performed to eliminate traces of genomic DNA. Real-time PCR was performed using CFX96 Real-Time PCR Detection System (Bio-Rad). PrecisionPLUS qPCR Mastermix with SYBR

Green (Primerdesign Ltd) was used to detect double-stranded DNA. Primer sequences are described in Table 1.

Behavioral tests

Experiments conformed to UK Home Office guidelines. Six mice/ genotype were tested. Mice were tested before surgery to ensure that there were no differences in normal responses between the genetic backgrounds. Tests were carried out as in Arthur-Farraj et al., 2012.

Statistical analysis

Results are expressed as mean ± SEM. Statistical significance was estimated by Student's t test, one-way ANOVA, two-way ANOVA, or Mann-Whitney U-test. A P value < 0.05 was considered as statistically significant. Statistical analysis was performed using GraphPad software (version 6.0).

Results

STAT3 activation is seen in embryonic nerves and persists in adult Schwann cells

Before studying the role of STAT3 in Schwann cells, we analysed STAT3 expression and activation during nerve development using Western blotting (Fig. 1A). STAT3 protein was present at all stages of the Schwann cell lineage from the Schwann cell precursor (SCP) stage at embryo day 12 (E12) onwards. At the precursor stage, serine 727 and tyrosine 705 STAT3 phosphorylation (P-STAT3-Ser727 and P-STAT3-Tyr705) were low and undetectable, respectively. At the immature Schwann cell stage (E18), both P-STAT3-Ser727 and P-STAT3-Tyr705 were clearly up-regulated and maintained until adulthood (Fig. 1A). Immunolabelling of teased adult nerves showed P-STAT3-Ser727 in the nucleus of both MBP-positive myelin cells and L1-positive non-myelin (Remak) cells (Fig. 1B), although the lower levels of P-STAT3-Tyr705 could not be detected unambiguously by this method. Thus,

STAT3 activation largely coincides with the Schwann cell precursor to Schwann cell transition, and basal STAT3 activation persists in adult nerves.

In WT mice, STAT3 does not have a major role in Schwann cell development and myelination

To explore the potential importance of STAT3 in the Schwann cell lineage we generated a conditional knock-out mouse in which STAT3 gene is specifically ablated only in Schwann cells. To do this $STAT3^{f/f}$ mice, having loxP sites flanking exons 12-14 of the STAT3 gene (Alonzi et al., 2001), were crossed with mice expressing Cre under the control of the P_0 promoter (Feltri et al., 2002), to generate P_0-Cre^{+}/$STAT3^{f/f}$ (STAT3cKO) mice (Fig. 2A).

The STAT3cKO mice were born and survived normally, and their nerves were indistinguishable from $control^{f/f}$ littermates (WT). At postnatal day three (P3), the area of a transverse section through the sciatic nerve, the number of Schwann cell nuclei/nerve, and the number of myelinated axons/nerve were similar in STAT3cKO and WT mice (Fig. 2B). In adult nerves, thick myelin sheaths were seen around the largest calibre axons and no significant difference was observed in the g-ratio between STAT3cKO and WT nerves (Fig. 2C).

The fact that Schwann cell numbers in the mutants were normal at P3 suggested that STAT3 signalling affected neither normal developmental death nor proliferation. This was confirmed by double labelling sections of P1.5 sciatic nerves with the proliferation marker Ki67 and SOX10 antibodies to identify Schwann cells. No significant difference was found in the number of Schwann cells labelled with Ki67 antibodies between WT and STAT3cKO nerves (Fig. 2D). In another test of proliferation, purified cultures of mouse Schwann cells were treated with βNRG-1, a well-established mitogen for Schwann cells in vitro, in the presence of a STAT3 peptide inhibitor. BrdU incorporation revealed that STAT3 inhibition had no effect on DNA synthesis of Schwann cells (Fig. 2E). The same results were also

seen using AG490, an inhibitor of the JAK2 signalling pathway (Nielsen et al., 1997) (data not shown).

Together these results suggest that the basal STAT3 activation in embryonic and postnatal Schwann cells is largely dispensable and has little developmental significance. In lens development, functional redundancy between STAT3 and STAT1 has been suggested (Ebong et al. 2004), but this issue remains unclear (Hirahara et al. 2015). Nevertheless, it remains possible that in a mouse in which STAT1 was genetically inactivated, a function for STAT3 in Schwann cell development might be revealed.

In injured nerves, STAT3 is activated to support Schwann cell survival

STAT3 signalling promotes survival in a number of cell types (e.g. Schweizer et al., 2002; Shen et al., 2004). To determine whether STAT3 supports Schwann cell survival in injured nerves, we examined STAT3 activation in cut sciatic nerves, and compared Schwann cell survival in cut nerves of WT and STAT3cKO mice. Western blots of cut nerves of adult WT mice showed a sharp (about eight-to-10 fold) rise in P-STAT3-Tyr705, the phosphorylation epitope that controls STAT3 dimerization and activation (Aaronson and Horvath, 2002). This was seen in nerve segments 0-2 mm and 2-7 mm distal to the cut at several time points, three, seven and 28 days, after injury (Fig. 3A). This STAT3 activation was not due to invading macrophages, because it was also seen in distal segments from cut nerves maintained in vitro for three days under conditions where macrophages are unable to invade (Fig. 3B). P-STAT3-Ser727, generally thought to modify signalling mediated by P-STAT3-Tyr705 (Decker and Kovarik, 2000), was also elevated after injury (Fig. 3A), and immunolabelling for both P-STAT3-Tyr705 and P-STAT3-Ser727 was seen in Schwann cell nuclei in teased injured nerves (Fig. 3C). In cultured nerve segments, however, Western blots failed to show P-STAT3-Ser727 up-regulation (Fig. 3B). This suggests that the activation of this epitope in Schwann cells after injury requires additional signals, which are

present in vivo but not in culture. Alternatively, it is possible that macrophages contribute significantly the signal measured in in vivo nerve homogenates (Girolami et al., 2010). In mice, nerve cut results in apoptotic Schwann cell death in the distal nerve stump. To test whether STAT3 supported the survival of Schwann cells after injury, we quantified dying cells in sections from sciatic nerves 3 days after cut using the TUNEL assay. This revealed a four-fold increase in the number of S100 positive TUNEL-labelled Schwann cells in STAT3cKO nerves compared with control nerves (Fig. 3D). Confirming this, an increase in the number of caspase-3 positive cells was also seen in cut STAT3cKO nerves (not shown).

To further test the idea that STAT3 is involved in the mechanisms that protect Schwann cells from death, we tested whether STAT3 protected cultured Schwann cells from stress induced by UV light, a model used to study STAT3 involvement in survival of other cell types (Shen et al., 2001; Sano et al., 2005). First, a UV-time course experiment determined that 24 hr was optimal for assessing cell death (data not shown). At this point, Schwann cell nuclei started to show the hallmarks of apoptosis (condensed, bright nuclei fragmenting into apoptotic bodies), but the cells were still attached to the coverslip allowing quantification by Hoechst staining. Using rat Schwann cells, we found that inhibition of STAT3 signalling by the JAK2 inhibitor AG490 increased UV-apoptosis (Fig. 4A). Conversely, enforced expression of a constitutively active form of STAT3 (STAT3-CA) protected Schwann cells from UV-induced death (Fig. 4B). Further, in mouse Schwann cells, UV light was more than twice as effective in inducing Schwann cell death in cells in which STAT3 had been genetically inactivated, compared to WT cells (Fig. 4C).

We conclude that activation of STAT3 signalling helps to protect Schwann cells in injured nerves from death.

STAT3 is required for long-term survival of repair Schwann cells after injury

Injury-related Schwann cell death has chiefly been studied in two situations. One is the acute death examined above, which represents a transient phase of a strong increase in apoptosis

from a very low level, in which a relatively small percentage of Schwann cell die (Grinspan et al., 1996; Yang et al., 2008; Ahmad et al., 2015). The other is the slow, large-scale death of Schwann cells that are deprived of axonal contact for long periods, often months, while axons regenerate towards them along the more proximal parts of the nerves. The loss of these chronically denervated Schwann cells is a major barrier to nerve repair in humans, and has been extensively studied in rodents (Höke, 2006; Sulaiman and Gordon, 2009).

Having found that STAT3 protects against acute death, we tested whether STAT3 also regulated the loss of chronically denervated Schwann cells. In these experiments we compared one, four, eight and 10 week cut nerves in mice in which the proximal stump was deflected to prevent regeneration into the distal nerve stump. First, Western blotting showed that in eight week cut nerves levels of P-STAT3-Tyr705 were only reduced by about 20-30% compared to those seen in one week cut nerves, in which P-STAT3-Tyr705 expression, in turn, is about eight-to-10 fold that in uninjured nerves (see earlier section). STAT3-Ser727 also remained activated in eight week cut nerves (Fig. 5A). This shows that the STAT3 pathway remains activated in chronically denervated Schwann cells, a precondition for the involvement of STAT3 in maintaining this cell population. Second, to test whether this was the case, electron microscopy was used to count the number of Schwann cell nuclei in the distal stumps of transected tibial nerves of WT and STAT3cKO mice at four, eight and 10 weeks after cut. This showed that in STAT3cKO nerves, the number of Schwann cells was substantially and significantly reduced compared with WT nerves at eight and 10 weeks (Fig. 5B). This result matched with the higher number of caspase-3 positive Schwann cells found in eight week cut nerves from STAT3cKO mice (Fig. 5D). At the earlier time point of four weeks, however, Schwann cell numbers were similar in both genotypes. The number of macrophages and fibroblasts was not significantly different in WT and mutant nerves at four and eight weeks after cut, while the number of fibroblasts was reduced in the mutant nerves at 10 weeks (Fig. 5B). Light microscopic counts of cells in the nerves of the fourth toe of WT and STAT3cKO mice four weeks and eight weeks after nerve cut (without reinnerveation)

showed similar reduction in cell numbers to that found in more proximal nerves (above and data not shown).

Our previous data on the regulation of Schwann cell proliferation had suggested that STAT3 signalling was not involved (see earlier section). This was confirmed by examining four day and four week cut nerves using cyclin D1 levels as a measure of proliferation (Atanasoski et al., 2001). At four days after cut, when proliferation is high, there was an equal and substantial rise in cyclin D1 levels in both WT and STAT3cKO nerves. Four weeks after cut, when proliferation is returning to baseline levels (Siironen et al., 1994; Hall, 1999) cyclin D1 levels were much lower and not significantly different between WT and mutants (Fig. 5C).

STAT3 is required for autocrine survival signalling in denervated Schwann cells

The experiments above indicated that STAT3 signalling supports the short- and long-term survival of Schwann cells after injury, an issue of particular importance for regeneration. We therefore examined the underlying mechanism. Previously, we suggested that the survival of Schwann cells in injured nerves depended on autocrine signalling involving IGF, NT-3 and PDGF-BB (Meier et al., 1999). We also showed that during development autocrine circuits appear at the immature Schwann cell stage (E18) and are not present in Schwann cell precursors, a developmental timing that the present work shows coincides with STAT3 activation. To test whether STAT3 signalling plays a role in Schwann cell autocrine survival circuits, we carried out experiments similar to those we used previously to identify autocrine Schwann cell mechanisms (Meier et al., 1999). First, to investigate the general ability of STAT3cKO cells to survive in culture without autocrine support (i.e. at low density), Schwann cells from P1 STATcKO and WT mice were plated at low density in simple defined medium (sDM). In a 48 hr assay, we found that the ability of STAT3cKO and WT cells to survive under these conditions was identical, both cells showing about 50% survival relative to the cell number present three hr after plating, which is in line with previous results (Meier et al., 1999) (Fig. 6A). When WT cells are plated at high density in this assay, their survival at 48 hr increases to about 80% due to autocrine factors secreted by the Schwann cells themselves

(Meier et al., 1999). To test whether these autocrine survival circuits functioned without STAT3, cells from P1 STATcKO and WT mice were plated at high density. The survival of WT cells at 48 and 72 hr increased to about 80% as expected (Fig.6B and C). The survival of STAT3cKO cells, however, remained similar to that seen in sparse cultures, suggesting absence of autocrine survival support (Fig. 6B and C).

In a further test of this, sparse cultures were exposed to conditioned defined medium (cDM) previously conditioned by dense Schwann cell cultures. As expected from an autocrine mechanism, and shown in previous work, this increased the survival of sparsely plated WT cells to levels similar to those seen in densely plated cultures. In contrast, the survival of sparsely plated STAT3cKO cells was not increased in response to conditioned medium, or to IGF-II, the major constituent of the conditioned medium (Meier et al. 1999) (Fig. 6D). This confirmed the absence of functioning autocrine survival circuits in STAT3cKO cells and indicated that these cells are not responsive to autocrine signals even when they are present in the culture medium. STAT3cKO cells remained, however, normally responsive to another key survival signal in the Schwann cell lineage, βNRG-1 that is expressed on axons and acts in a paracrine manner, since βNRG-1 was equally effective in supporting the survival of E13 Schwann cell precursors from WT and STAT3cKO mice (Fig. 6E).

To determine whether autocrine Schwann cell signals activate endogenous STAT3 signalling, we used an adenoviral STAT3-luciferase GFP reporter construct containing four tandem copies of STAT3 binding sites (Besser et al., 1999, Staples et al., 2007) (Fig. 6F). The construct was infected into neonatal rat Schwann cell cultures prior to exposure to relevant components. Because low density cultures generated insufficient luciferase signal, higher cell densities were used in these experiments, although this generated high background readings, even in control cultures without added factors, presumably due to the presence of autocrine factors. Nevertheless, elevated luciferase signal, indicating STAT3 activation, was obtained in response to Schwann cell conditioned medium, a combination of low concentrations of IGF-II , NT-3 and PDGF-BB that mimics the conditioned medium

401 (Meier et al., 1999), or high concentration of the major conditioned medium ingredient IGF-II
402 (Fig. 6F).

403 These results show that STAT3 is required for autocrine Schwann cell survival signalling,
404 and suggest that defective autocrine survival support contributes to the substantial loss of
405 STAT3cKO Schwann cells when these cells are subjected to chronic denervation.

406 **STAT3 is essential for the long-term maintenance of the phenotype of repair**
407 **Schwann cells**

408 The gradual loss of repair supportive capacity by distal nerves is due not only to the death of
409 chronically denervated Schwann cells, but also to the gradual fading of the repair Schwann
410 cell phenotype, evidenced by the gradual reduction in expression of regeneration supportive
411 factors such as GDNF and BDNF in distal nerve stumps during chronic denervation (Höke et
412 al., 2002; Eggers et al., 2010). We therefore asked whether STAT3 might be more broadly
413 involved in maintaining the regeneration supportive functions of injured nerves by testing
414 whether STAT3 was required for the maintenance of the repair Schwann cell phenotype, in
415 addition to supporting the long-term survival of these cells. To this end we compared the
416 repair Schwann cell phenotype in eight week cut distal stumps of WT and STAT3cKO nerves
417 using morphometric analysis of regeneration tracks (Bungners bands), qRT-PCR, and
418 Western blotting.

419 Morphologically, the regeneration tracks in STAT3cKO nerves were obviously abnormal.
420 Compared to eight week cut WT nerves, there were fewer cellular profiles in each track, the
421 profiles were flatter, and the average area of each profile was increased. The number of
422 redundant basal lamina profiles was also higher, a feature likely to reflect the increased cell
423 death in these nerves (see previous section) (Fig. 7A-E).

424 Analysis of eight week cut STAT3cKO nerves by qRT-PCR also showed substantial
425 reduction in expression of key markers of repair Schwann cells, such as c-Jun, Olig1, and
426 Shh, and repair-supportive factors such as GDNF and BDNF (Fig.7F), all of which are

activated in Schwann cells after injury (Shy et al. 1996; Arthur-Farraj et al. 2012; Fontana et al. 2012; Brushart et al. 2013).

Western blotting showed that eight weeks after cut, STAT3cKO nerves expressed lower levels of c-Jun and GAP-43 proteins compared to WT (Fig. 7, G and H). Two other proteins that are up-regulated after injury, N-Cadherin and p75NTR were expressed at levels similar to those seen in eight week cut WT nerves (Fig. 7I).

While repair Schwann cells were clearly abnormal in eight week cut STAT3cKO sciatic nerves, short-term denervated cells in these mice were relatively normal (Fig. 8). Thus in four week cut nerves the morphological changes that were obvious at eight weeks were detectable but mild (Fig. 7A). In one week cut nerves, c-Jun mRNA and protein were found at normal levels in STAT3cKO mice. Expression of N-Cadherin and p75NTR protein was also similar in WT and STAT3cKO mice (Fig. 8A-C). In these nerves, the substantial difference in GAP-43 levels seen at eight weeks was only emerging (Fig. 7H). In line with these findings, functional tests of regeneration of the sciatic nerve after crush injury indicated that nerve repair, which in these assays takes place during the first two-to-three weeks after injury, proceeds at a similar rate in WT and STAT3cKO mice (Fig. 8D-F).

We conclude that STAT3 has a dual role in injured nerves. It supports the long-term survival of repair Schwann cells and is required for the long-term maintenance of the repair Schwann cell phenotype. In contrast, STAT3 appears relatively unimportant for the initial generation of repair Schwann cells.

Discussion

Because human nerves are long and axons grow slowly, all but the most distal nerve injuries result in chronic denervation of Schwann cells that can last for months, even years. In experimental animals long-term denervation of the distal stump can be mimicked by nerve cut combined with deflection of the proximal stump to prevent reinnervation. Clinical

observations and animal experiments agree that axon-free distal nerve stumps gradually lose the capacity to support regeneration. Although this is considered a key reason for regeneration failure in humans, and is known to involve loss of trophic factor expression and cell death, the molecular signalling mechanisms underlying this deterioration remain obscure (Höke, 2006; Sulaiman and Gordon, 2009; Jonsson et al., 2013). In the present work, we (i) report that STAT3 is activated by Tyr705 phosphorylation in Schwann cells distal to nerve injury in agreement with previous work by others, (ii) show that this activation is sustained in repair Schwann cells during long-term denervation, and (iii) demonstrate that selective inactivation of Schwann cell STAT3 results not only in a marked loss of Schwann cells from chronically denervated distal stumps, but also reduces the capacity of these cells to maintain their repair-supportive phenotype. This identification of a transcriptional mechanism involved in supporting long-term survival and differentiation of repair Schwann cells contributes to our understanding of how these important cells are maintained, and will help identify in molecular terms the failures that lead to their deterioration.

The present data indicate that STAT3 regulates Schwann cell survival, a function likely to be particularly significant for the long-term survival of Schwann cells in denervated distal stumps. This is in line with the role of STAT3 in other systems (e.g. Bader et al., 2014). We find that absence of STAT3 results in increased Schwann cell death in four different situations. First, this is seen in the STAT3cKO Schwann cells of chronically denervated distal nerves. Second, increased death is also seen STAT3cKO nerves three days after injury although in this case relatively few Schwann cells die, and Schwann cell numbers are not significantly different between STAT3 mutants and WT controls (Grinspan et al., 1996; Yang et al., 2008; Ahmad et al., 2015). Third, STAT3 inactivation results in reduced response to autocrine survival signals in neonatal cultured Schwann cells. Fourth, STAT3 knockout cells die more readily in response to UV irradiation.

STAT3 signalling does not appear to affect developmental death of Schwann cells, where we have previously shown that TGFβ signalling plays a role (D'Antonio et al., 2006) and it is

not involved in Schwann cell precursor survival controlled by NRG-1. Although STAT3 signalling promotes proliferation in some systems (e.g. Debidda et al., 2005), we do not find this effect in Schwann cells. Taken together our results suggest that the significant loss of repair Schwann cells in chronically denervated distal stumps of STAT3cKO mice is caused by a defective autocrine support, a survival mechanism that we and others have suggested to be central for preventing death of Schwann cells without axonal contact (Dowsing et al., 1999; Meier et al., 1999).

Using qRT-PCR analysis of the distal stump eight weeks after nerve cut, we find that STAT3cKO mice show decreased expression of key markers of repair Schwann cells compared with levels seen in WT mice at the same time points. This includes *c-Jun, Olig1* and *Shh* and of neurotrophic factors, such as *GDNF* and *BDNF* known to promote axonal regeneration. With respect to protein expression, GAP-43 and c-Jun levels were also lower while N-Cadherin and p75NTR levels were the same in mutant and control distal stumps. This is significant because p75NTR promotes cell death in Schwann cells after nerve injury (Ferri and Bisby, 1999) but cannot be a defining factor in the increased death seen in STAT3 mutant distal stumps.

The importance of STAT3 signalling in the Schwann cells of long-term denervated nerves is also seen at the morphological level. In STAT3cKO mice the shape of repair cells and structure of the regeneration tracks they form (bands of Bungner) is clearly altered, although not to the same extent as that seen in Schwann cell c-Jun null nerves (Parkinson et al., 2008; Arthur-Farraj et al., 2012). The number of Schwann cell profiles per Bungner band is also lower. This is likely to reflect the increased cell death in the mutants, but changes in cell shape could also contribute to this effect.

Elevation in STAT3 expression in injured nerves has been reported previously. Rapid activation of STAT3 signalling is implicated in the retrograde signalling from severed axons to the neuronal soma and in the initiation of axonal growth (Bareyre et al., 2011; Ben-Yaakov et al., 2012; Chandran et al., 2016). An increase in STAT3 signalling is also seen in

Schwann cells after peripheral nerve injury. Sheu et al. (2000) used Western blotting to show activation of STAT3 Ser 727 in the proximal nerve stump from 30 min to 16 days after injury, in agreement with results above that show strong activation of STAT3 in axons after sciatic nerve transection. More modest activation was seen in the distal stump 3 hr and 24 hr after nerve transection, most likely in Schwann cells. This finding was supported by Lee et al. (2009b) who showed activation of Ser727 in the sciatic nerve distal stump between 6 h and five days after crush injury and in cultured Schwann cells. In Schwann cells, IL-6, acting via gp130, and NRG-1 acting via ErbB2/3 can both induce STAT3 activation on Ser727 and Tyr705. IL-6, acting via STAT3 is also required for early induction of GFAP after nerve injury (Lee et al*.,* 2009a; Lee et al., 2009b).

We have shown previously, using immunohistochemistry, that GAP-43 levels in Schwann cells in the sciatic nerve rise slowly in the weeks after nerve injury (Curtis et al., 1992), although a rapid rise in GAP-43 levels is seen in terminal Schwann cells of the neuromuscular junction (Woolf et al., 1992). This is confirmed in the present study, which shows that in WT nerves protein levels of GAP-43 are higher at eight weeks than at one week after nerve cut. In STAT3cKO nerves, however, levels of GAP-43 are substantially lower than those in WT, both at one week and, more strikingly, at eight weeks after cut, suggesting that in Schwann cells STAT3 regulates GAP-43 levels. This is in line with that seen in other cell types, including neurons and astrocytes. In neurons, GAP-43 elevation after conditioning lesion depends on STAT3 and is promoted by the cytokine IL-6, which is also expressed at elevated levels in denervated Schwann cells (Hung et al., 2016). In astrocytes STAT3 activation is involved in the activation of GAP-43 that occurs during astrogliosis (Cafferty et al., 2004; Qui et al., 2005).

The prevention of the phenotypic deterioration and death of chronically denervated repair Schwann cells are two important goals in the effort to improve the outcomes after nerve injury. It is encouraging in this context that there is evidence, albeit limited, that the loss of the repair-supportive phenotype may be reversible. In rat Schwann cells, a reduction on the

expression of c-erbB receptors and p75NTR due to long-term denervation can be restored in vitro by exposing the cells to NRG-1 (Li et al., 1998). When chronically denervated cells that have reduced growth supportive capacity are treated in vitro with TGFβ, a factor expressed by macrophages and denervated Schwann cells, the regenerative support provided by these cells increases when they are tested in an in vivo grafting experiment (Sulaiman and Gordon, 2002). It has also been shown that engineered expression in Schwann cells of genes encoding particular growth associated factors can promote axon growth in vivo (Hoyng et al., 2014).

Although individual proteins will play a prominent role (Fontana et al., 2012), the exceptional capacity of repair Schwann cells to support regeneration is likely due to the integrated action of many components, including cell surface and secreted factors and morphology. The identification of pathways and signals, including transcription factors, which determine this repair phenotype opens the way towards pharmacological interventions that co-ordinately up-regulate the repair programme and therefore provide a favourable way of promoting nerve repair. c-Jun is one such signal, since the striking elevation of Schwann cell c-Jun after injury acts as a global amplifier of the repair phenotype, without which regeneration is seriously curtailed (Arthur-Farraj et al., 2012). The question of whether c-Jun is also involved in the log-term maintenance of repair Schwann cells is under investigation. The present work identifies STAT3 as the second transcription factor that regulates the repair cell. Although STAT3 is less involved in the initial reprogramming of myelin and Remak cells to repair cells, it has a significant role in long-term denervated distal stumps, where STAT3 maintains the differentiation state of repair Schwann cells, and supports their survival. In future work it will be of interest to explore this pathway and related signalling molecules for their potential to promote regeneration.

References

560 Aaronson DS, Horvath CM (2002) A road map for those who don't know JAK-STAT. Science
561 296(5573):1653-1655.

562 Ahmad I, Fernando A, Gurgel R, Clark JJ, Xu L, Hansen MR (2015) Merlin status regulates
563 p75(NTR) expression and apoptotic signaling in Schwann cells following nerve injury.
564 Neurobiol Dis 82:114-122.

565 Akagi K, Sandig V, Vooijs M, Van der Valk M, Giovannini M, Strauss M, Berns A (1997) Cre-
566 mediated somatic site-specific recombination in mice. Nucleic Acids Res 25:1766-1773.

567 Allan CH (2000) Functional results of primary nerve repair. Hand Clin 16: 67–67.

568 Alonzi T, Maritano D, Gorgoni B, Rizzuto G, Libert C, Poli V (2001) Essential role of STAT3
569 in the control of the acute-phase response as revealed by inducible gene inactivation
570 [correction of activation] in the liver. Mol Cell Biol 21:1621-1632.

571 Arthur-Farraj PJ, Latouche M, Wilton DK, Quintes S, Chabrol E, Banerjee A, Woodhoo A,
572 Jenkins B, Rahman M, Turmaine M, Wicher GK, Mitter R, Greensmith L, Behrens A, Raivich
573 G, Mirsky R, Jessen KR (2012) c-Jun reprograms Schwann cells of injured nerves to
574 generate a repair cell essential for regeneration. Neuron 75:633-647.

575 Atanasoski S, Shumas S, Dickson C, Scherer SS, Suter U (2001) Differential cyclin D1
576 requirements of proliferating Schwann cells during development and after injury.Mol Cell
577 Neurosci 18:581-592.

578 Bader AM, Brodarac A, Klose K, Bieback K, Choi YH, Kang KS, Kurtz A, Stamm C (2014)
579 Cord blood mesenchymal stromal cell-conditioned medium protects endothelial cells via
580 STAT3 signaling. Cell Physiol Biochem 34:646-657.

581 Bareyre FM, Garzorz N, Lang C, Misgeld T, Büning H, Kerschensteiner M (2011) In vivo
582 imaging reveals a phase-specific role of STAT3 during central and peripheral nervous
583 system axon regeneration. Proc Natl Acad Sci USA 108:6282-6287.

584 Ben-Yaakov K, Dagan SY, Segal-Ruder Y, Shalem O, Vuppalanchi D, Willis DE, Yudin D,
585 Rishal I, Rother F, Bader M, Blesch A, Pilpel Y, Twiss JL, Fainzilber M (2012) Axonal
586 transcription factors signal retrogradely in lesioned peripheral nerve. EMBO J 31:1350-1363.

587 Besser D, Bromberg JF, Darnell JE Jr, Hanafusa H (1999) A single amino acid substitution
588 in the v-Eyk intracellular domain results in activation of Stat3 and enhances cellular
589 transformation. Mol Cell Biol 19:1401-1409.

590 Bromberg JF, Wrzeszczynska MH, Devgan G, Zhao Y, Pestell RG, Albanese C, Darnell JE
591 Jr (1999) Stat3 as an oncogene. Cell 98:295-303.

592 Brosius Lutz A, Barres BA (2014) Contrasting the glial response to axon injury in the central
593 and peripheral nervous systems. Dev Cell 28:7-17.

594 Brushart TM, Aspalter M, Griffin JW, Redett R, Hameed H, Zhou C, Wright M, Vyas A, Höke
595 A (2013) Schwann cell phenotype is regulated by axon modality and central-peripheral
596 location, and persists in vitro. Exp Neurol 247:272-281.

597 Cafferty WBJ, Gardiner NJ, Das P, Qiu J, McMahon SB, Thompson SW (2004) Conditioning
598 injury-induced spinal axon regeneration fails in interleukin-6 knockout mice. J Neurosci
599 24:4432-4443.

600 Chandran V et al (2016) A systems-level analysis of the Peripheral Nerve intrinsic axonal
601 growth program. Neuron 89:956-970.

602 Chen ZL, Yu WM, Strickland S (2007). Peripheral regeneration. Annu Rev Neurosci 30:209–
603 233.

604 Curtis R, Stewart HJ, Hall SM, Wilkin GP, Mirsky R, Jessen KR (1992) GAP-43 is expressed
605 by nonmyelin-forming Schwann cells of the peripheral nervous system. J Cell Biol 116:1455-
606 1464.

607 D'Antonio M, Droggiti A, Feltri ML, Roes J, Wrabetz L, Mirsky R, Jessen KR (2006)
608 TGFbeta type II receptor signaling controls Schwann cell death and proliferation in
609 developing nerves. J Neurosci 26:8417-8427.

610 Debidda M, Wang L, Zang H, Poli V, Zheng Y (2005) A role of STAT3 in Rho GTPase-
611 regulated cell migration and proliferation. J Biol Chem 280:17275-17285.

612 Decker T, Kovarik P (2000) Serine phosphorylation of STATs. Oncogene 19:2628-2637.

613 Dong Z, Sinanan A, Parkinson D, Parmantier E, Mirsky R, Jessen KR (1999) Schwann cell
614 development in embryonic mouse nerves. J Neurosci Res 56:334-348.

615 Dowsing BJ, Morrison WA, Nicola NA, Starkey GP, Bucci T, Kilpatrick TJ (1999). Leukemia
616 inhibitory factor is an autocrine survival factor for Schwann cells. J Neurochem 73:96-104.

617 Ebong S, Chepelinsky AB, Robinson ML, Zhao H, Yu CR, Egwuagu CE (2004)
618 Characterization of the roles of STAT1 and STAT3 signal transduction pathways in
619 mammalian lens development. Mol Vis. 10:122-131.

620 Eggers R, Tannemaat MR, Ehlert EM, Verhaagen J (2010) A spatio-temporal analysis of
621 motoneuron survival, axonal regeneration and neurotrophic factor expression after lumbar
622 ventral root avulsion and implantation. Exp Neurol 223:207-220.

623 Feltri ML, Graus Porta D, Previtali SC, Nodari A, Migliavacca B, Cassetti A, Littlewood-
624 Evans A, Reichardt LF, Messing A, Quattrini A, Mueller U, Wrabetz L (2002) Conditional
625 disruption of beta 1 integrin in Schwann cells impedes interactions with axons. J Cell Biol
626 156:199-209.

627 Ferri CC, Bisby MA (1999) Improved survival of injured sciatic nerve Schwann cells in mice
628 lacking the p75 receptor. Neurosci Lett 272:191-194.

629 Fontana X, Hristova M, Da Costa C, Patodia S, Thei L, Makwana M, Spencer-Dene B,
630 Latouche M, Mirsky R, Jessen KR, Klein R, Raivich G, Behrens A (2012) c-Jun in Schwann

631 cells promotes axonal regeneration and motoneuron survival via paracrine signalling. J Cell
632 Biol 198:127–141.

633 Girolami EI, Bouhy D, Haber M, Johnson H, David S (2010) Differential expression and
634 potential role of SOCS1 and SOCS3 in Wallerian degeneration in injured peripheral nerve.
635 Exp Neurol 223:173-182.

636 Glenn TD, Talbot WS (2013) Signals regulating myelination in peripheral nerves and the
637 Schwann cell response to injury. Curr Opin Neurobiol 23:1041-1048.

638 Gomez-Sanchez JA, Carty L, Iruarrizaga-Lejarreta M2, Palomo-Irigoyen M, Varela-Rey M,
639 Griffith M, Hantke J, Macias-Camara N, Azkargorta M, Aurrekoetxea I, De Juan VG,
640 Jefferies HB, Aspichueta P, Elortza F, Aransay AM, Martínez-Chantar ML, Baas F, Mato JM,
641 Mirsky R, Woodhoo A, Jessen KR (2015) Schwann cell autophagy, myelinophagy, initiates
642 myelin clearance from injured nerves. J Cell Biol 210:153-168.

643 Grinspan JB, Marchionni MA, Reeves M, Coulaloglou M, Scherer SS (1996) Axonal
644 interactions regulate Schwann cell apoptosis in developing peripheral nerve: neuregulin
645 receptors and the role of neuregulins. J Neurosci 16:6107-6118.

646 Hall SM (1999) The biology of chronically denervated Schwann cells. Ann N Y Acad Sci
647 883:215-233.

648 Hirahara K, Onodera A, Villarino AV, Bonelli M, Sciumè G, Laurence A, Sun HW, Brooks
649 SR, Vahedi G, Shih HY, Gutierrez-Cruz G, Iwata S, Suzuki R, Mikami Y, Okamoto Y,
650 Nakayama T, Holland SM, Hunter CA, Kanno Y, O'Shea JJ (2015) Asymmetric action of
651 STAT transcription factors drives transcriptional outputs and cytokine specificity. Immunity
652 42:877-889.

653 Höke A, Gordon T, Zochodne DW, Sulaiman OA (2002) A decline in glial cell-line-derived
654 neurotrophic factor expression is associated with impaired regeneration after long-term
655 Schwann cell denervation. Exp Neurol 173:77–85.

656 Höke A (2006) Neuroprotection in the peripheral nervous system: rationale for more effective
657 therapies. Arch Neurol 63:1681-1685.

658 Hoyng SA, De Winter F, Gnavi S, de Boer R, Boon LI, Korvers LM, Tannemaat MR, Malessy
659 MJ, Verhaagen J (2014) A comparative morphological, electrophysiological and functional
660 analysis of axon regeneration through peripheral nerve autografts genetically modified to
661 overexpress BDNF, CNTF, GDNF, NGF, NT3 or VEGF. Exp Neurol 261:578-593.

662 Hung CC, Lin CH, Chang H, Wang CY, Lin SH, Hsu PC, Sun YY, Lin TN, Shie FS, Kao LS,
663 Chou CM, Lee YH (2016) Astrocytic GAP43 Induced by the TLR4/NF-κB/STAT3 axis
664 attenuates astrogliosis-mediated microglial activation and neurotoxicity. J Neurosci 36:2027-
665 2043.

666 Inserra MM, Bloch DA, Terris DJ (1998). Functional indices for sciatic, peroneal, and
667 posterior tibial nerve lesions in the mouse. Microsurgery 18:119-124.

668 Jaegle M, Ghazvini M, Mandemakers W, Piirsoo M, Driegen S, Levavasseur F, Raghoenath
669 S, Grosveld F, Meijer D (2003) The POU proteins Brn-2 and Oct-6 share important functions
670 in Schwann cell development. Genes Dev 17:1380-1391.

671 Jessen KR, Brennan A, Morgan L, Mirsky R, Kent A, Hashimoto Y, Gavrilovic J. (1994) The
672 Schwann cell precursor and its fate: a study of cell death and differentiation during
673 gliogenesis in rat embryonic nerves. Neuron 12:509-527.

674 Jessen KR, Mirsky R (2016) The repair Schwann cell and its function in regenerating nerves.
675 J Physiol 594:3521-3531.

676 Jessen KR, Mirsky R, Arthur-Farraj P (2015) The role of cell plasticity in tissue repair:
677 adaptive cellular reprogramming. Dev Cell 34:613-620.

678 Jonsson S, Wiberg R, McGrath AM, Novikov LN, Wiberg M, Novikova LN, Kingham PJ
679 (2013) Effect of delayed peripheral nerve repair on nerve regeneration, Schwann cell
680 function and target muscle recovery. PLoS One 8:e56484.

681 Klein D, Groh J, Wettmarshausen J, Martini R (2014) Nonuniform molecular features of
682 myelinating Schwann cells in models for CMT1: distinct disease patterns are associated with
683 NCAM and c-Jun upregulation. Glia 62:736-750.

684 Lee HK, Seo IA, Suh DJ, Hong JI, Yoo YH, Park HT (2009a) Interleukin-6 is required for the
685 early induction of glial fibrillary acidic protein in Schwann cells during Wallerian
686 degeneration. J Neurochem 108(3):776-786.

687 Lee HK, Jung J, Lee SH, Seo SY, Suh DJ, Park HT (2009b) Extracellular signal-regulated
688 kinase activation is required for Serine 727 phosphorylation of STAT3 in Schwann Cells in
689 vitro and in vivo. Korean J Physiol Pharmacol. 13:161-168.

690 Li H, Wigley C, Hall SM (1998) Chronically denervated rat Schwann cells respond to GGF in
691 vitro. Glia 24:290-303.

692 Lundborg G (2000) A 25-year perspective of peripheral nerve surgery: evolving
693 neuroscientific concepts and clinical significance. J Hand Surg Am 25:391–414.

694 Meier C, Parmantier E, Brennan A, Mirsky R, Jessen KR (1999) Developing Schwann cells
695 acquire the ability to survive without axons by establishing an autocrine circuit involving
696 insulin-like growth factor, neurotrophin-3, and platelet-derived growth factor-BB. J Neurosci
697 19:3847-3859.

698 Michalski B, Bain JR, Fahnestock M (2008) Long-term changes in neurotrophic factor
699 expression in distal nerve stump following denervation and reinnervation with motor or
700 sensory nerve. J Neurochem 105:1244-1252.

701 Morgan L, Jessen KR, Mirsky R (1991) The effects of cAMP on differentiation of cultured
702 Schwann cells: progression from an early phenotype (04+) to a myelin phenotype (P0+,
703 GFAP-, N-CAM-, NGF-receptor-) depends on growth inhibition. J Cell Biol 112:457-467.

704 Nielsen M, Kaltoft K, Nordahl M, Röpke C, Geisler C, Mustelin T, Dobson P, Svejgaard A,
705 Odum N (1997) Constitutive activation of a slowly migrating isoform of Stat3 in mycosis

706 fungoides: tyrphostin AG490 inhibits Stat3 activation and growth of mycosis fungoides tumor
707 cell lines. Proc Natl Acad Sci USA 94:6764-6769.

708 Parkinson DB, Bhaskaran A, Arthur-Farraj P, Noon LA, Woodhoo A, Lloyd AC, Feltri ML,
709 Wrabetz L, Behrens A, Mirsky R, Jessen KR (2008) c-Jun is a negative regulator of
710 myelination. J Cell Biol 181:625-637.

711 Parkinson DB, Bhaskaran A, Droggiti A, Dickinson S, D'Antonio M, Mirsky R, Jessen KR
712 (2004) Krox-20 inhibits Jun-NH2-terminal kinase/c-Jun to control Schwann cell proliferation
713 and death. J Cell Biol 164:385-394.

714 Parkinson DB, Dong Z, Bunting H, Whitfield J, Meier C, Marie H, Mirsky R, Jessen KR
715 (2001) Transforming growth factor beta (TGFbeta) mediates Schwann cell death in vitro and
716 in vivo: examination of c-Jun activation, interactions with survival signals, and the
717 relationship of TGFbeta-mediated death to Schwann cell differentiation. J Neurosci 21:8572-
718 8585.

719 Qiu J, Cafferty WB, McMahon SB, Thompson SW (2005) Conditioning injury-induced spinal
720 axon regeneration requires signal transducer and activator of transcription 3 activation. J
721 Neurosci 25:1645-1653.

722 Sano S, Chan KS, Kira M, Kataoka K, Takagi S, Tarutani M, Itami S, Kiguchi K, Yokoi M,
723 Sugasawa K, Mori T, Hanaoka F, Takeda J, DiGiovanni J (2005) Signal transducer and
724 activator of transcription 3 is a key regulator of keratinocyte survival and proliferation
725 following UV irradiation. Cancer Res 65:5720-5729.

726 Scheib J, Höke A (2013) Advances in peripheral nerve regeneration. Nat Rev Neurol 9:668-
727 676.

728 Schweizer U1, Gunnersen J, Karch C, Wiese S, Holtmann B, Takeda K, Akira S, Sendtner M
729 (2002) Conditional gene ablation of Stat3 reveals differential signalling requirements for
730 survival of motoneurons during development and after nerve injury. J Cell Biol 156:287-297.

731 Shen Y, Devgan G, Darnell JE Jr, Bromberg JF (2001) Constitutively activated Stat3
732 protects fibroblasts from serum withdrawal and UV-induced apoptosis and antagonizes the
733 proapoptotic effects of activated Stat1. Proc Natl Acad Sci USA 98:1543-1548.

734 Shen Y1, Schlessinger K, Zhu X, Meffre E, Quimby F, Levy DE, Darnell JE Jr (2004)
735 Essential role of STAT3 in postnatal survival and growth revealed by mice lacking STAT3
736 serine 727 phosphorylation. Mol Cell Biol 24:407-419.

737 Sheu JY, Kulhanek DJ, Eckenstein FP (2000). Differential patterns of ERK and STAT3
738 phosphorylation after sciatic nerve transection in the rat. Exp Neurol 166:392-402.

739 Shy ME, Shi Y, Wrabetz L, Kamholz J, Scherer SS (1996) Axon-Schwann cell interactions
740 regulate the expression of c-jun in Schwann cells. J Neurosci Res 43:511-525.

741 Siironen J, Collan Y, Röyttä M (1994) Axonal reinnervation does not influence Schwann cell
742 proliferation after rat sciatic nerve transection. Brain Res 654:303-311.

743 Staples KJ, Smallie T, Williams LM, Foey A, Burke B, Foxwell BM, Ziegler-Heitbrock L
744 (2007) IL-10 induces IL-10 in primary human monocyte-derived macrophages via the
745 transcription factor Stat3. J Immunol 178:4779-4785.

746 Sulaiman OA, Gordon T (2002) Transforming growth factor-beta and forskolin attenuate the
747 adverse effects of long-term Schwann cell denervation on peripheral nerve regeneration in
748 vivo. Glia 37:206-218.

749 Sulaiman OA, Gordon T (2009) Role of chronic Schwann cell denervation in poor functional
750 recovery after nerve injuries and experimental strategies to combat it. Neurosurgery 65(4
751 Suppl): A105-114.

752 Sulaiman W, Gordon T (2013) Neurobiology of peripheral nerve injury, regeneration, and
753 functional recovery: from bench top research to bedside application. Ochsner J 13:100-108.

754 Turkson J, Ryan D, Kim JS, Zhang Y, Chen Z, Haura E, Laudano A, Sebti S, Hamilton AD,
755 Jove R (2001) Phosphotyrosyl peptides block Stat3-mediated DNA binding activity, gene
756 regulation, and cell transformation. J Biol Chem 276:45443-45455.

757 Wanner IB, Anderson MA, Song B, Levine J, Fernandez A, Gray-Thompson Z, Ao Y,
758 Sofroniew MV (2013) Glial scar borders are formed by newly proliferated, elongated
759 astrocytes that interact to corral inflammatory and fibrotic cells via STAT3-dependent
760 mechanisms after spinal cord injury. J Neurosci 33:12870–12886.

761 Weinberg HJ, Spencer PS (1978) The fate of Schwann cells isolated from axonal contact. J
762 Neurocytol 7:555-569.

763 Woodhoo A, Alonso MB, Droggiti A, Turmaine M, D'Antonio M, Parkinson DB, Wilton DK, Al-
764 Shawi R, Simons P, Shen J, Guillemot F, Radtke F, Meijer D, Feltri ML, Wrabetz L, Mirsky
765 R, Jessen KR (2009). Notch controls embryonic Schwann cell differentiation, postnatal
766 myelination and adult plasticity. Nat Neurosci 12:839-847.

767 Woolf CJ, Reynolds ML, Chong MS, Emson P, Irwin N, Benowitz LI (1992) Denervation of
768 the motor endplate results in the rapid expression by terminal Schwann cells of the growth-
769 associated protein GAP-43. J Neurosci 12:3999-4010.

770 Yang DP, Zhang DP, Mak KS, Bonder DE, Pomeroy SL, Kim HA (2008) Schwann cell
771 proliferation during Wallerian degeneration is not necessary for regeneration and
772 remyelination of the peripheral nerves: axon-dependent removal of newly generated
773 Schwann cells by apoptosis. Mol Cell Neurosci 38:80-88.

774 You S, Petrov T, Chung P H, Gordon T (1997). The expression of the low affinity nerve
775 growth factor receptor in long-term denervated Schwann cells. Glia 20:87–100.

776

777

778 **Figure legends**

779 FIGURE 1. Basal activation of STAT3 takes place early in Schwann cell development and
780 persists in the adult

781 (A) Western blots showing total STAT3 and its phosphorylated forms in sciatic nerve extracts
782 from WT control mice at different developmental stages. STAT3 is present throughout the
783 Schwann cell lineage. P-STAT3-Ser727 is found at very low levels in Schwann cell
784 precursors (E12) but its expression increases at the immature Schwann cell stage and is
785 maintained in adulthood. PSTAT3-Tyr705 is expressed at lower levels and seen from the
786 immature Schwann cell stage (E18) onwards. GAPDH is used as a loading control.

787 (B) Fibres in teased sciatic nerve preparations showing P-STAT3-Ser727 immunoreactivity
788 in Schwann cell nuclei, (red; upper two panels) also stained with DAPI (lower two panels).
789 The two left hand panels show a non-myelinated (Remak) fibre, identified by L1 antibodies.
790 The right hand panels shows a myelinated fibre, identified by MBP antibodies. Scale bar:
791 25µm.

792

793

794 FIGURE 2. STAT3 appears dispensible for Schwann cell development and myelination.

795 (A) Cre-mediated deletion of the STAT3 gene in Schwann cells. PCR analysis for STAT3
796 gene deletion in DNA extracts from tail and sciatic nerve of adult genetically wild-type (gWT),
797 $STAT3^{f/f}$ (f/f) and P_0-$Cre^{+}STAT3^{f/f}$ (cKO) mice. Amplification of the gWT allele results in a
798 210bp fragment while $STAT3^{f/f}$ allele containing the loxP sites generates a bigger band
799 (370bp). The deleted allele generates a 310bp fragment. Specific recombination is absent
800 from the tail of cKO mice, but present in cKO sciatic nerve where Cre recombinase is
801 expressed under the control of the P_0 gene. Successful deletion in the STAT3 gene was also
802 detected in DNA samples from P8 purified Schwann cell cultures from STAT3cKO mice.

(B) Electron micrographs from P3 sciatic nerves of WT and STAT3cKO mice showing normal nerve morphology and no apparent abnormalities of myelination in the mutant. Graphs show quantification of number of nuclei per transverse nerve section (top), nerve area (middle), and number of axons starting to be myelinated (bottom) in WT and STAT3cKO nerves. n=5 mice of each genotype. Data are presented as mean ± SEM. Scale bar: 1μm.

(C) Electron micrographs from adult sciatic nerves of WT and STAT3cKO mice showing normal myelin profiles in the mutant. The graph shows g-ratio analysis; the differences in g-ratios are not significant. n=4 of each genotype. Data are presented as mean ± SEM. Scale bar: 1μm.

(D) Ki67 immunolabelling showing similar Schwann cell proliferation in P1.5 sciatic nerves of WT and STAT3cKO mice. Transverse nerve sections were double labelled for SOX10 and Ki67. The graph shows the percentage of $Ki67^{+}SOX10^{+}$ cells relative to total number of $SOX10^{+}$ cells, showing no differences between groups. n=4 for each genotype. Data are presented as mean ± SEM. Scale bar: 25μm.

(E) BrdU immunolabelling showing that inhibition of STAT3 has no significant effect on Schwann cell proliferation induced by βNRG-1. Cultured, purified Schwann cells from WT mice were treated with βNRG-1 (20ng/ml) for 48 hr to stimulate proliferation with BrdU included for the last 24 hr. The experiment was carried out in the presence of vehicle or a STAT3 peptide inhibitor. The graph shows the percentage of $BrdU^{+}$ nuclei relative to the number of Hoechst-stained nuclei. n=4 for each genotype. Data are presented as mean ± SEM. Scale bar: 50μm.

Figure 3. STAT3 activation after injury promotes Schwann cell survival

(A) Western blots showing the up-regulation of P-STAT3-Tyr705 and P-STAT3-Ser727 distal to injury in uncut, as well as in 3, 7 and 28 day cut sciatic nerves from WT mice. The

829 measurements were carried out on 2 and 5 mm segments measured from the cut site as
830 indicated. Densitometric quantification of Western blots shows the percentage of activitation
831 in cut relative to uncut nerves. n= a minimum of four mice per time point. Data are presented
832 as mean ± SEM and analysed by one-way ANOVA. **, P < 0.01; ***, P < 0.001; *** P<
833 0.0001 (cut vs. uncut).

834 (B) Western blots comparing WT tibial nerve segments mantained in vitro for 3 days, to
835 uninjured WT nerves. Note activation of P-STAT3-Tyr705 in the segments, while P-STAT3-
836 Ser727 levels remain as in uninjured nerves. Graphs show the percentage of activation in
837 segments relative to uninjured nerves. n=5. Data are presented as mean ± SEM and
838 analysed by Mann-Whitney U test. **, P < 0.01.

839 (C) Teased fibres of 3 day cut nerves from WT control mice labeled with P-STAT3-Tyr705
840 and P-STAT3-Ser727 antibodies. Positive immunostaining is localised in Schwann cell
841 nuclei. DAPI labels nuclei. Scale bar: 50μm.

842 (D) TUNEL labelling of sections from the distal stump of sciatic nerve sections 3 days after
843 cut. Note higher percentage of apoptotic nuclei in STAT3cKO mice compared to WT
844 controls. Arrows indicate TUNEL-positive nuclei. Graph shows percentage of TUNEL/S100-
845 positive cells in the Hoechst/S100-positive Schwann cell population. n=4 for each genotype.
846 Data are presented as mean ± SEM and analysed by Mann-Whitney U test. *, P < 0.05.
847 Scale bar: 20μm.

848

849

850 Figure 4. STAT3 protects Schwann cells from apoptosis after 24 hr exposure to UV light.

851 (A) Graph shows higher percentage of apoptotic nuclei in rat Schwann cells treated with
852 AG490 (25 μM) to inhibit JAK2/STAT3 signalling compared with vehicle. n=3 for each

genotype. Data are presented as mean ± SEM and analysed by two-way ANOVA. **, P < 0.01.

(B) Graph shows lower percentage of cell apoptosis in rat Schwann cells expressing a constitutively active form of STAT3 (STAT3-CA). Cultured Schwann cells were co-transfected with STAT3-CA or an empty vector (pRcCMV) and GFP. n=5 for each genotype. Data are presented as mean ± SEM and analysed by 2-way ANOVA. ****, P < 0.0001.

(C) Graph showing percentage of apoptotic nuclei in $STAT3^{f/f}$ mouse Schwann cells infected with a control GFP- (WT) or Cre-expressing (STAT3cKO) adenovirus. Note that Cre-mediated deletion of the STAT3 gene in $STAT3^{f/f}$ Schwann cells increased the percentage of UV-induced apoptosis. n=5 for each genotype. Data are presented as mean ± SEM and analysed by 2-way ANOVA. ****, P < 0.0001.

FIGURE 5. STAT3 promotes long-term survival of Schwann cells after nerve injury.

(A) Western blots of uncut, and of 1 and 8 week cut nerves in WT mice showing that P-STAT3-Tyr705 and P-STAT3-Ser727 remain elevated at 8 weeks although the levels are somewhat lower than at one week. Densitometric quantification shows the percentage of activation in 8 week cut nerves relative to one week cut nerves. n=3 for each genotype. Data are presented as mean ± SEM and analysed by Wilcoxon's signed rank test. *, P< 0.05.

(B) Graphs showing the number of cell nuclei per transverse section of the tibial nerve. Electron micrographs of WT and STAT3cKO tibial nerves 5mm distal to injury were used to identify and count cell types at 4 weeks (n=3), 8 weeks (n=7) and 10 weeks (n=6) after sciatic nerve transection. The upper panels show reduced number of Schwann cell nuclei in STAT3cKO tibial nerves 8 and 10 weeks after injury. The lower panels show no differences

878 in macrophage number, but 10 week cut nerves from STAT3cKO mice had reduced
879 numbers of fibroblasts. Data are presented as mean ± SEM and analysed by Mann-Whitney
880 U test. *, P< 0.05; **, P<0.01 (STAT3cKO vs WT).

881 (C) Western blots showing no differences in cyclin D1 expression in 4 day and 4 week
882 STAT3cKO cut nerves compared to WT nerves. GAPDH is used as a loading control. Graph
883 shows the densitometric analysis of the Western blot. Each value is normalised to that seen
884 in 4 day cut WT nerves. n=4 for each condition. Data are presented as mean ± SEM.

885 (D) Graphs showing higher caspase-3 expression in 8 week cut nerves from STAT3cKO
886 mice than in WT mice. n=4 for WT and n=3 for STAT3cKO. Data are presented as mean ±
887 SEM and analysed by Mann-Whitney U test. *, p<0.05.

888

889 FIGURE 6. STAT3 is required for normal autocrine surival signalling by denervated Schwann
890 cells.

891 (A) Without autocrine support (at low density, 200 cells/400µl of medium) STAT3cKO and
892 WT Schwann cells show similar 48 hr survival in sDM without serum. Survival is expressed
893 as a percentage of cells present on sister coverslips 3 hr after plating. n=3. Data are
894 presented as mean ± SEM.

895 (B) Hoechst staining shows nuclei of Schwann cells from P1 WT and STAT3cKO nerves
896 cultured at high density (4000 cells/400µl of medium) in sDM without serum for 3 and 48 hr
897 Note reduced cell numbers in STAT3cKO cultures at 48 hr Scale bar: 50µm.

898 (C) With autocrine support (at high density, 4000 cells/400µl) STAT3cKO Schwann cells
899 survive poorly at 48 and 72 hr compared with WT cells. The cells were cultured in sDM
900 without serum. Survival is expressed as in (A). n=3. Data are presented as mean ± SEM and
901 analysed by two-way ANOVA. ***, P< 0.001 (STAT3cKO vs WT).

(D) Graph showing that low density WT cultures respond to conditioned medium, or IGF-II at high concentration (100ng/ml) by increase in survival at 48 hr (compare to A). Note that STAT3cKO cultures do not show this response. n=3. Data are presented as mean ± SEM and analysed by 2-way ANOVA. ****, P< 0.0001 (WT vs STAT3cKO).

(E) WT and STAT3cKO Schwann cell precursors are equally responsive to the survival signal βNRG-1. Schwann cell precursors were dissected from STAT3cKO and WT E13 mouse embryos and cultured for 24 hr with or without βNRG-1 (20 ng/ml). Survival was assessed as in (A). n=4. Data are presented as mean ± SEM and analysed by two-way ANOVA. ****, P< 0.0001 (βNRG-1 treated vs untreated).

(F) The micrograph shows cultured rat Schwann cells infected with the STAT3-Luc-GFP adenovirus (green) and Hoechst nuclear staining (blue). The graph shows luciferase fluorescence, indicative of STAT3 activation, in response to 48 hr exposure to conditioned médium, the combination of IGF-II (1.6ng/ml), NT3 (0.8ng/ml) and PDGF-BB (0.8ng/ml) that mimics the conditioned medium, or high concentration of IGF-II (100ng/ml). The activation is expressed relative to the signal obtained from control medium. n=6 for conditioned medium and n=12 for the combination of IGF-II, NT3 and PDGF-BB and high concentration of IGF-II. Data are presented as mean ± SEM and analysed by Kruskal-Wallis test. *, P< 0.05; ***, P< 0.001. Scale bar: 10μm.

FIGURE 7. STAT3 is requried for the maintenance of the repair Schwann cell phenotype

(A) Electron micrographs showing transverse sections of WT and STAT3cKO distal stumps at 4 and 8 weeks after transection (without regeneration). Note abnormal morphology of the regeneration tracks (Bungner`s bands) in 8 week STAT3cKO nerves compared to 8 week WT controls. The right hand panels show higher power micrographs from STAT3cKO nerves illustrating redundant basal lamina (asterisks) and regeneration tracks containing a single

(one arrow) or a few (double arrow) Schwann cell profiles, enclosed by a basal lamina. Scale bar: 1µm. Morphometric analysis of 8 week cut nerves is presented in B-E.

(B) The number of Schwann cell profiles per Bungner band is reduced by more than half in 8 week cut STAT3cKO nerves. n=3. Data are presented as mean ± SEM and analysed by Mann-Whitney U test. ****, P< 0.0001.

(C) Schwann profiles in STAT3cKO regeneration tracks lose their roundness and become flatter. n=3. Data are presented as mean ± SEM and analysed by Mann-Whitney U test. ****, P< 0.0001.

(D) The average area of Schwann cell profiles in STAT3cKO nerves is larger than in WT nerves. n=3. Data are presented as mean ± SEM and analysed by Mann-Whitney U test. ****, P< 0.0001.

(E) STAT3cKO nerves show 6-fold increase in the number of redundant basal laminae compared to WT samples. n=3. Data are presented as mean ± SEM and analysed by Mann-Whitney U test. ****, P< 0.0001.

(F) qRT-PCR analysis showing significantly lower mRNA expression of the repair Schwann cell genes *c-Jun, Olig1, Shh, GDNF* and *BDNF*, in 8 week cut distal nerves from STAT3cKO mice compared to WT controls. A pool of 9 WT and STAT3cKO distal stumps were used for RNA extraction. n=3. Data are presented as mean ± SEM and analysed by Mann-Whitney U test. *, P< 0.05.

(G) Western blots showing lower expression of c-Jun in 8 week cut nerves from STAT3cKO mice compared to WT controls. n=4 for each genotype. Data are presented as mean ± SEM and analysed by Mann-Whitney U test. *, P< 0.05.

(H) Western blots showing lower expression of GAP-43 in 8 week cut nerves from STAT3cKO mice compared to WT controls. Shown also are the relatively low GAP-43 levels 1 week after cut in both genotypes. Graphs show the densitometric analysis of Western blots

relative to WT uncut. n=4 for each genotype. Data are presented as mean ± SEM and analysed by two-way ANOVA.***, P< 0.001.

(I) Western blots showing similar levels of p75NTR and N-Cadherin in 8 week cut nerves WT and STAT3cKO mice. n=4 for each genotype. Graphs show the densitometric analysis of Western blots relative to WT uncut. Data are presented as mean ± SEM.

FIGURE 8. STAT3 is not required for the initial generation of the repair Schwann cell phenotype

(A) qRT-PCR analysis shows that one week after cut c-Jun expression in WT and STAT3cKO nerves is similar. RNA was extracted from one week cut nerves using a pool of 2 distal stumps from STAT3cKO and WT mice for each experiment. n=4. Data are presented as mean ± SEM.

(B) Western blots showing similar c-Jun protein levels in one week cut WT and STAT3cKO nerves. Graphs show the densitometric analysis of Western blots relative to WT uncut. n=4 mice for each genotype. Data are presented as mean ± SEM.

(C) Western blots showing no differences in the expression of N-Cadherin and p75NTR proteins in WT and STAT3cKO nerves one week after cut. Graphs show the densitometric analysis of Western blots relative to WT uncut. n=4 mice for each genotype. Data are presented as mean ± SEM.

(D) Walking track analysis to quantify sensory-motor function following sciatic nerve injury. Sciatic function index (SFI; Inserra et al 1998), which assesses nerve-mediated function of the hind limb by measuring toe spread and print length of hind paw footprints, showed similar values for WT and STAT3cKO mice before and, significantly, after nerve injury. The right hand panel shows representative examples of footprints from uninjured mice and at different times after injury as indicated. Note the increased print length and decreased toe

977 spread after peripheral nerve lesion in both mouse lines ui: uninjured. n=6. Data are
978 presented as mean ± SEM.

979 (E) Toe spread reflex measurements show no significant differences in recovery of motor
980 function between WT and STAT3cKO mice. n=6. Data are presented as mean ± SEM.

981 (F) Toe pinch test for sensory function shows no significant differences between WT and
982 STAT3cKO mice in the percentage of mice responding to pinching distal parts of toes 3, 4
983 and 5 after sciatic nerve lesion. n=6. Data are presented as mean ± SEM.

984

985

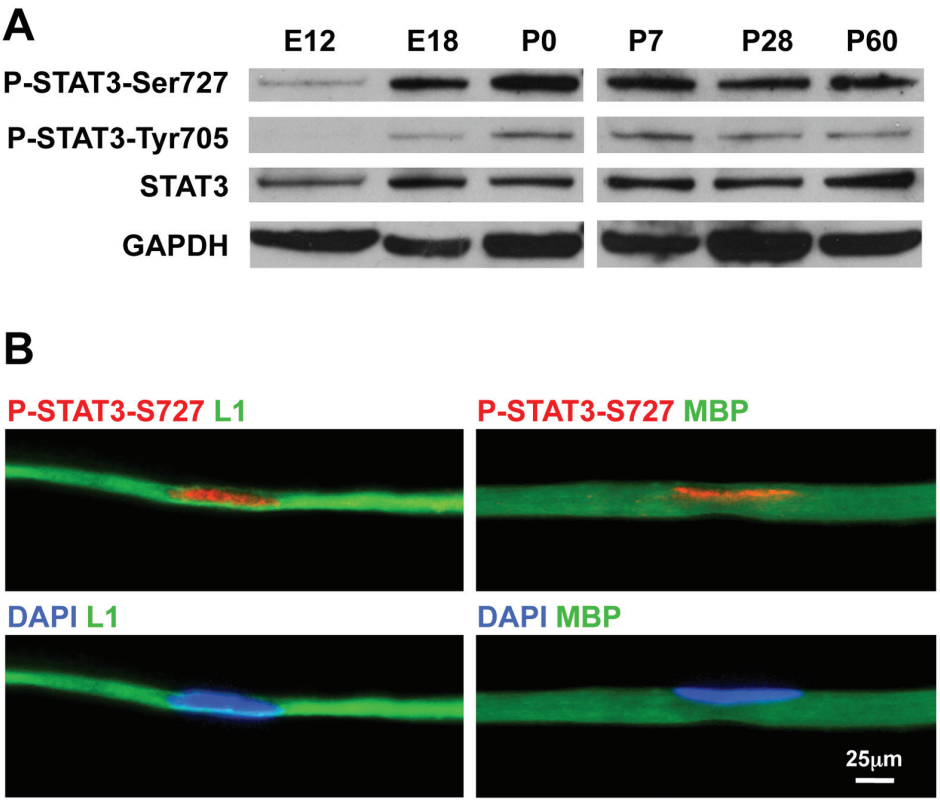

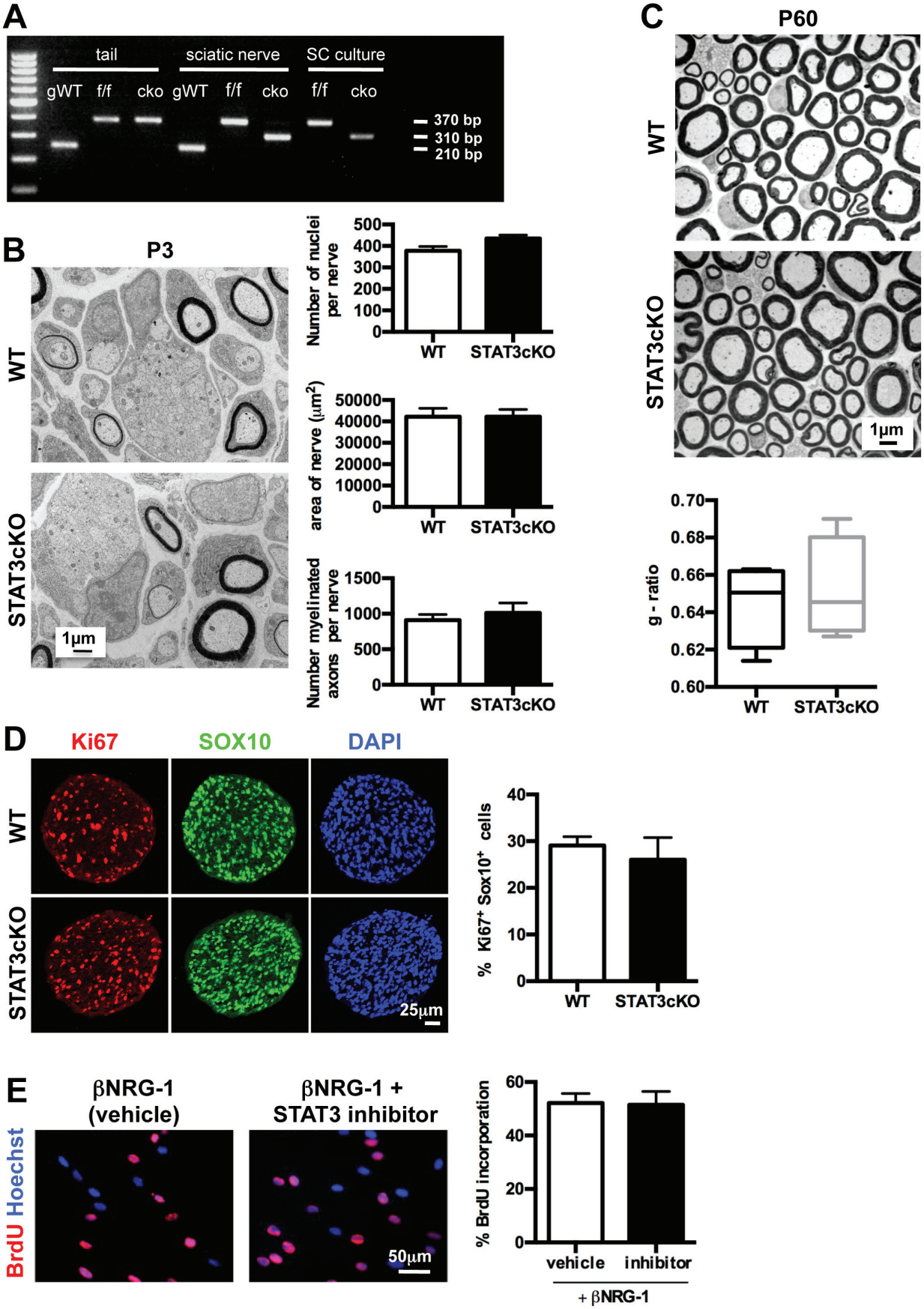

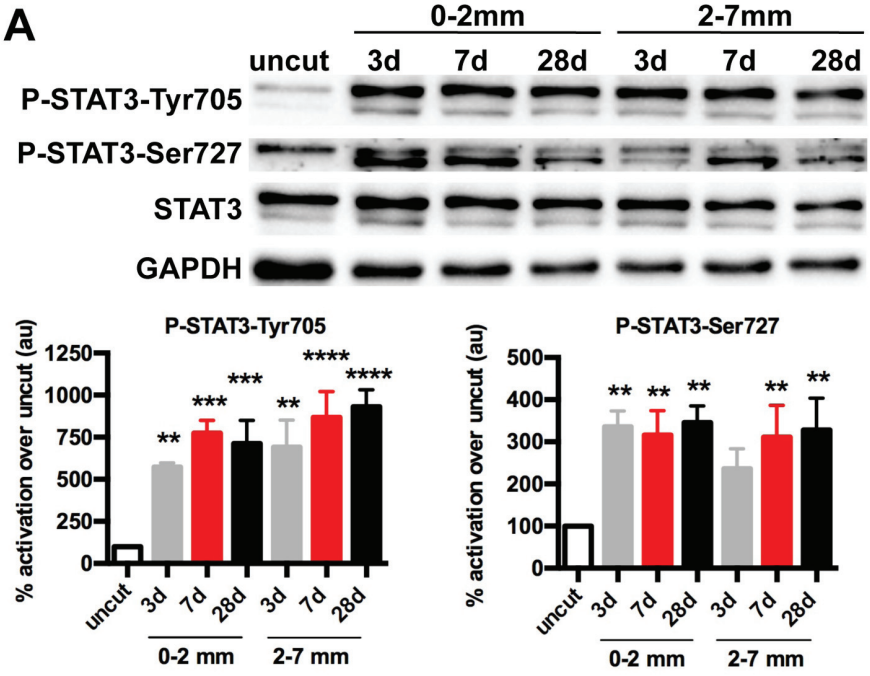

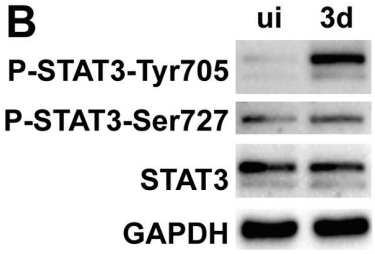

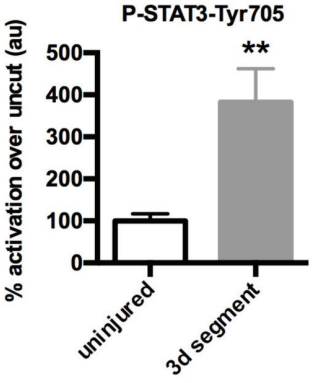

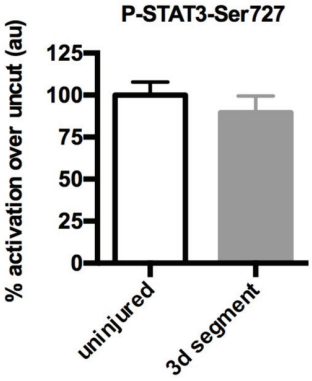

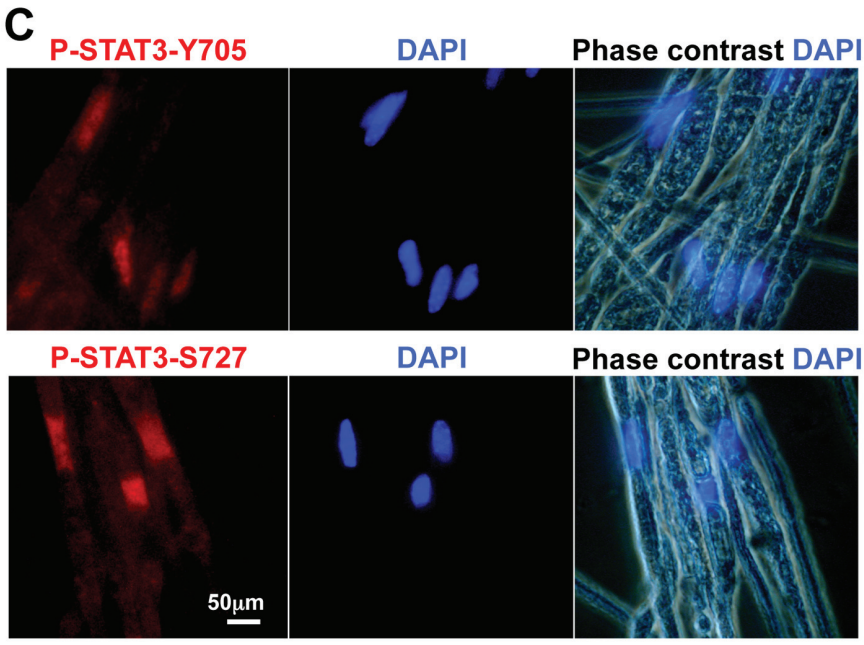

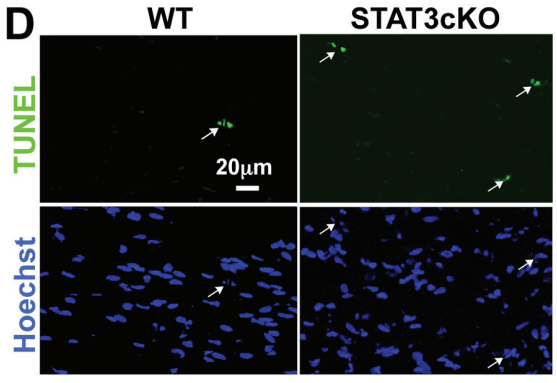

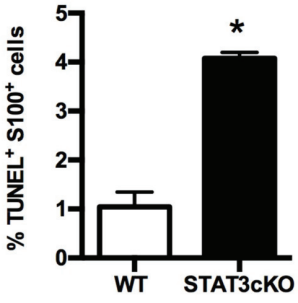

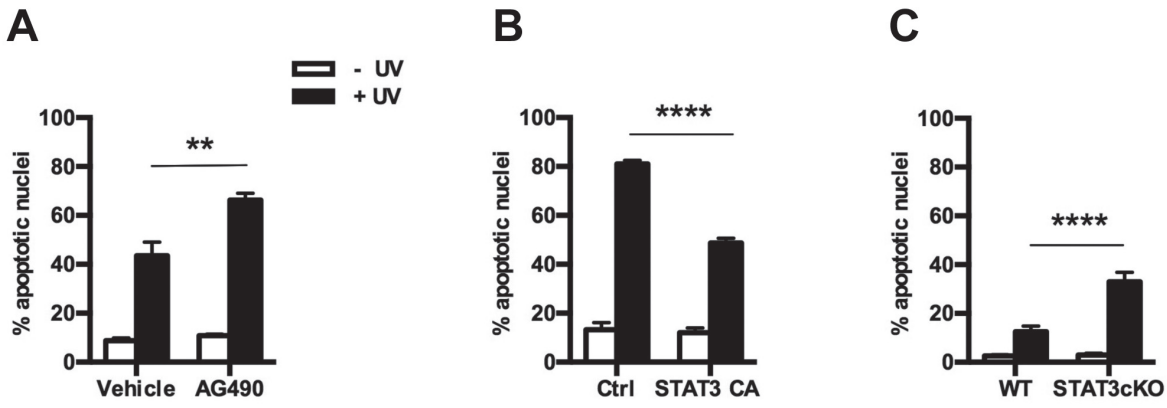

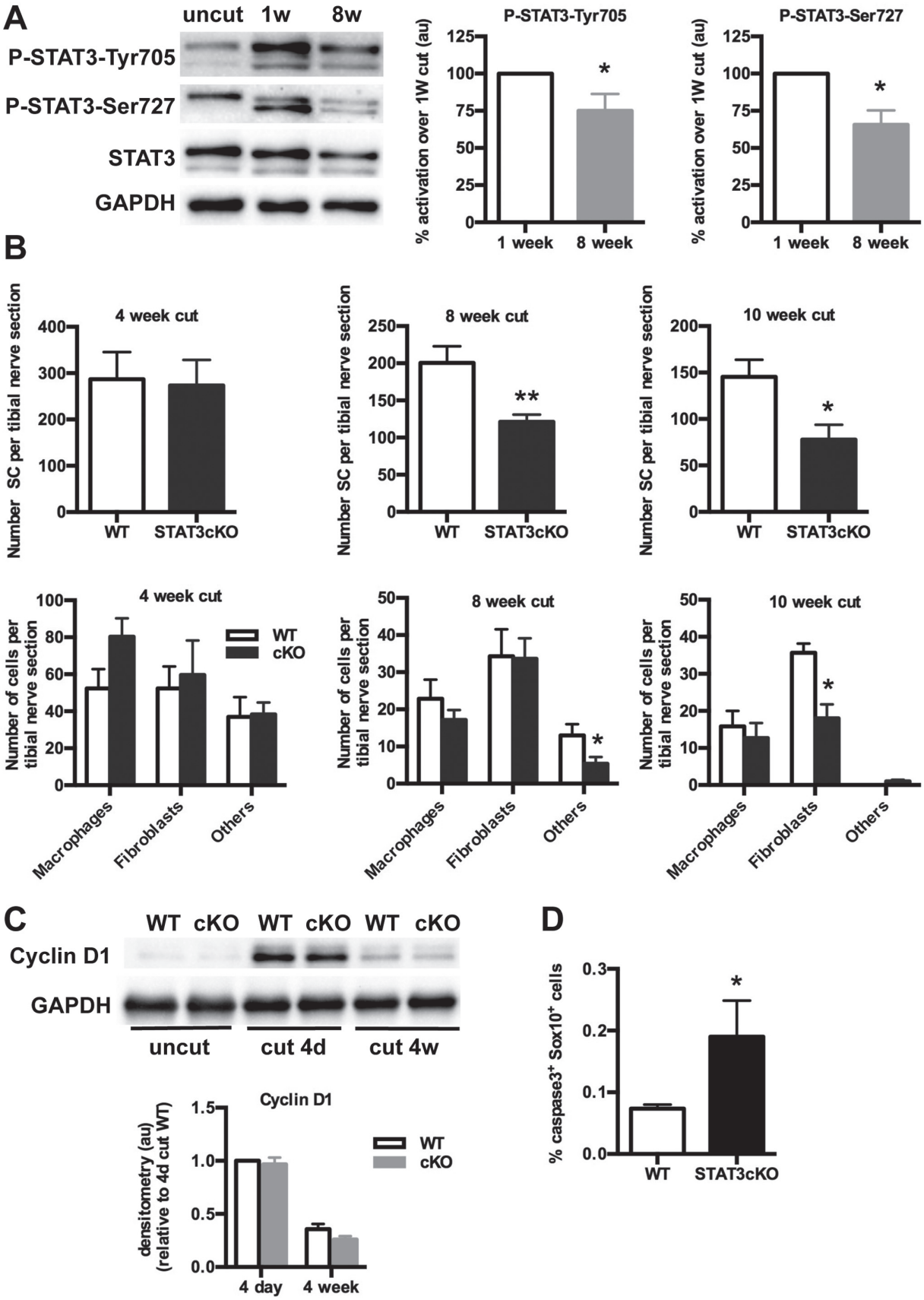

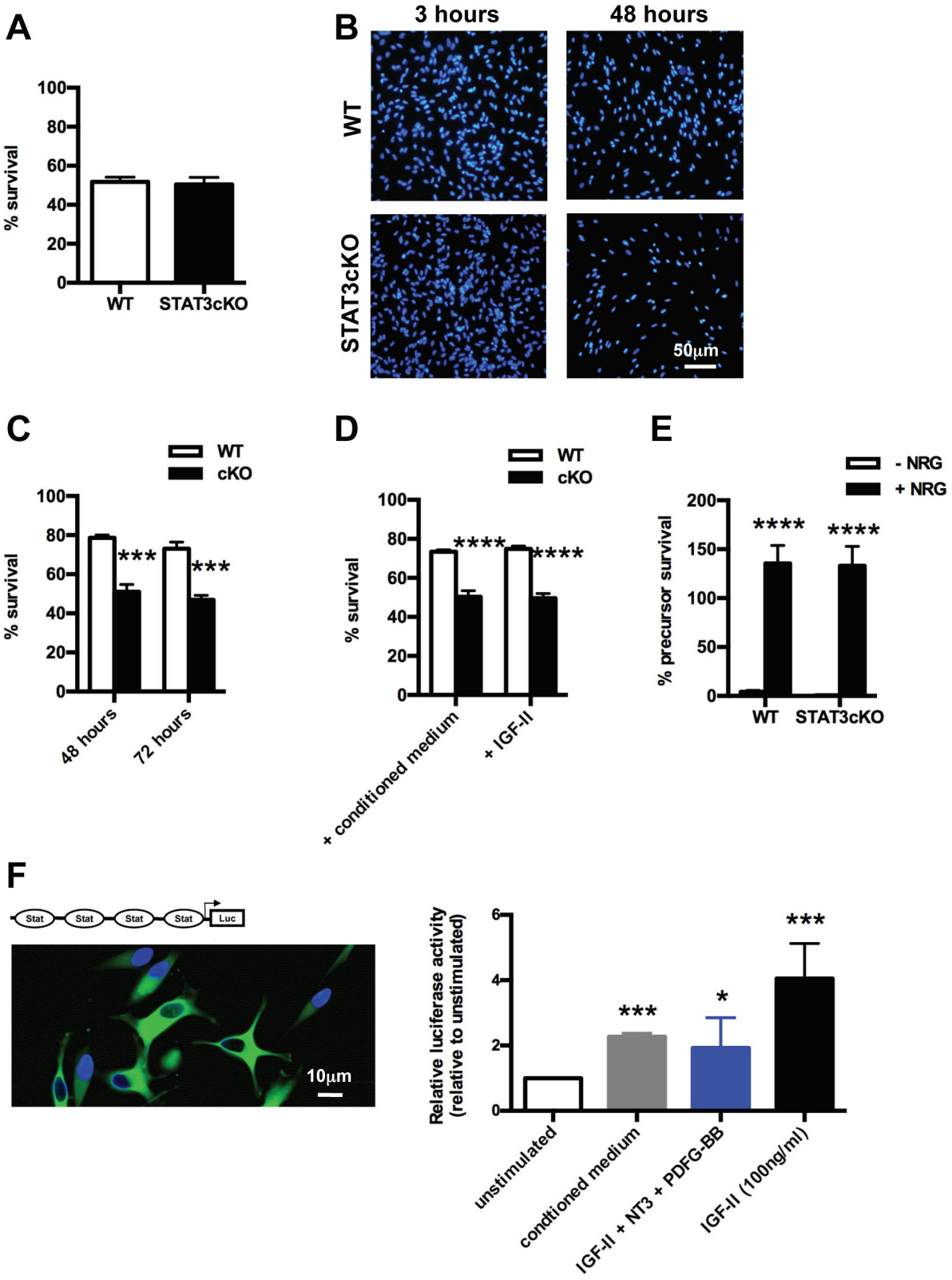

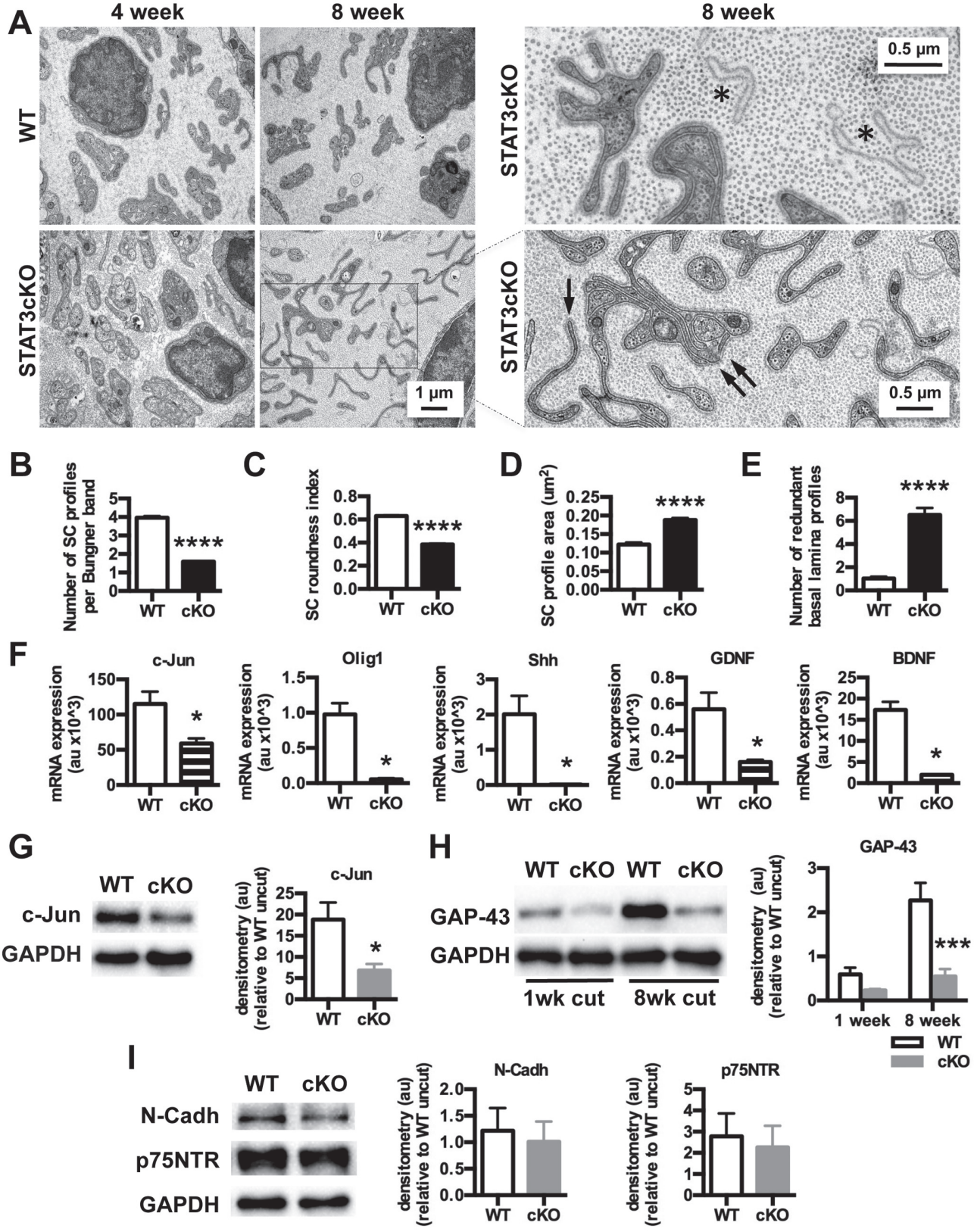

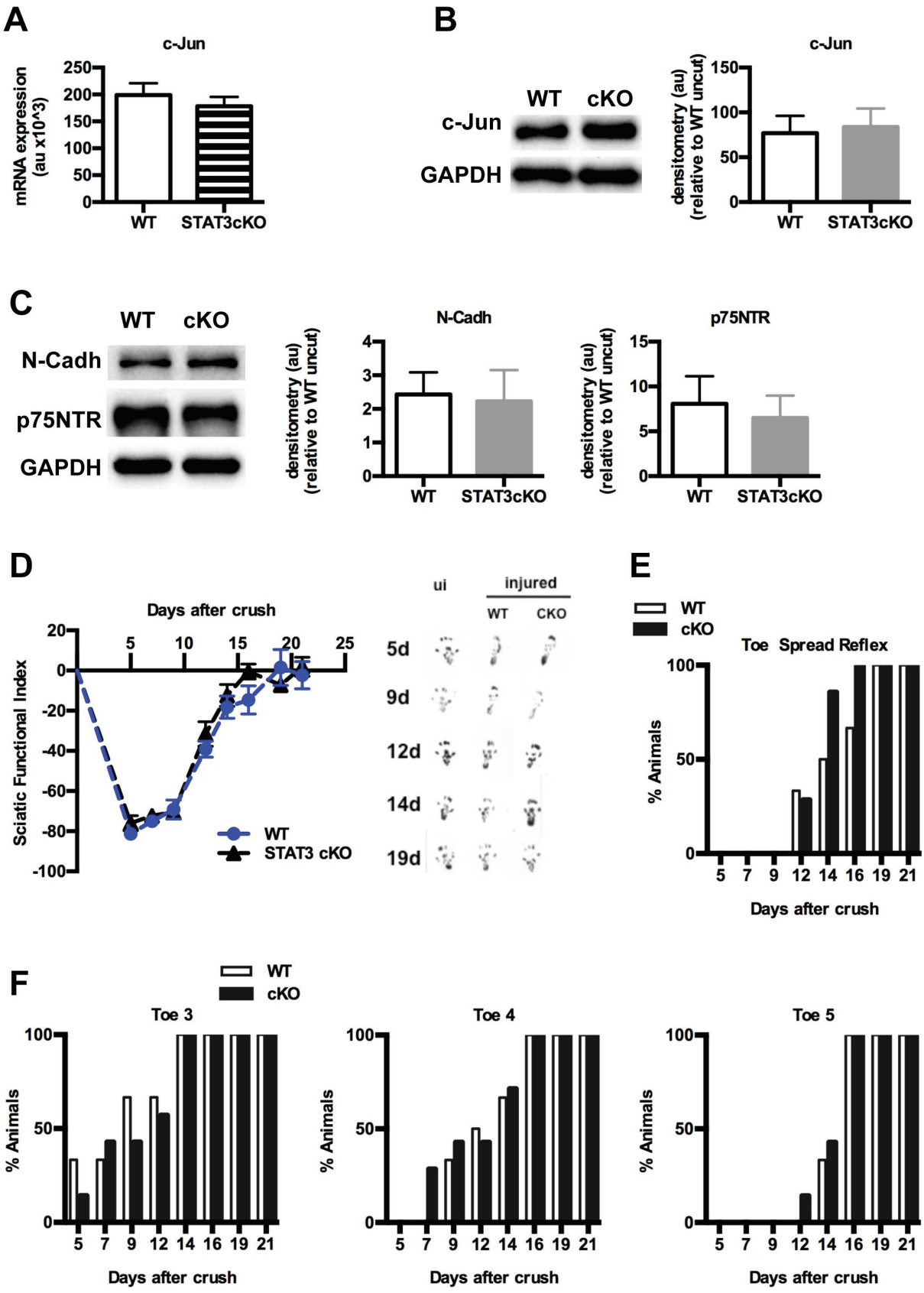

Table 1. Primers for qPCR and genotyping

Gene		Accession	Sense sequence	Antisense sequence
	Glyceraldehyde-3-phosphate dehydrogenase	NM_001289726.1	AGGTCGGTGTGAACGGATTTG	TGTAGACCATGTAGTTGAGGTCA
Canx	Calnexin	NM_007597.3	CAACAGGGGAGGTTTATTTTGCT	TCCCACTTTCCATCATATTTGGC
c-Jun	c-Jun	NM_010591.2	CCTTCTACGACGATGCCCTC	GGTTCAAGGTCATGCTCTGTTT
Olig1	Oligodendrocyte transcription factor 1	NM_016968.4	CCGCCCCAGATGTACTATGC	AACCCACCAGCTCATACAGC
Shh	Sonic hedgehog	NM_009170.3	AAAGCTGACCCCTTTAGCCTA	TTCGGAGTTTCTTGTGATCTTCC
GDNF	Glial cell-derived neurotrophic factor	NM_010275.3	GATTCGGGCCACTTGGAGTT	GACAGCCACGACATCCCATA
BDNF	Brain-derived neurotrophic factor	NM_007540.4	TCATACTTCGGTTGCATGAAGG	AGACCTCTCGAACCTGCCC

Primers used for qPCR

Primers used for genotyping STAT3f/f mice

5'-CAC CAA CAC ATG CTA TTT GTA GG-3' and 5'-CCT GTC TCT GAC AGG CCA TC-3' (210-bp band for WT allele and 370-bp band flox allele). Primers for the STAT3 deleted flox allele (310-bp band) were 5'-CAC CAA CAC ATG CTA TTT GTA GG-3' and 5'-GCA GCA GAA TAC TCT ACA GCT C-3'. The primers for the P0-Cre transgene were 5′-GCTGGCCCAAATGTTGCTGG-3′ and 5′-CCACCACCTCTCCATTGCAC-3′ (480-bp band; Feltri et al., 2002).